Geochemistry, Geophysics, Geosystems®

AGU ADVANCING EARTH AND SPACE SCIENCE

RESEARCH ARTICLE
10.1029/2022GC010663

Breaking Up Is Hard to Do: Magmatism During Oceanic Arc Breakup, Subduction Reversal, and Cessation

James Gill[1], Erin Todd[2], Kaj Hoernle[3], Folkmar Hauff[3], Allison Ann Price[4], and Matthew G. Jackson[4]

[1]Department of Earth and Planetary Sciences, University of California, Santa Cruz, CA, USA, [2]U.S. Geological Survey, Alaska Science Center, Anchorage, AK, USA, [3]GEOMAR Helmholtz Centre for Ocean Research, Kiel, Germany, [4]Department of Earth Science, University of California, Santa Barbara, CA, USA

Abstract The formerly continuous Vitiaz Arc broke into its Vanuatu and Fijian portions during a reversal of subduction polarity in the Miocene. Basaltic volcanism in Fiji that accompanied the breakup ranged from shoshonitic to low-K and boninitic with increasing distance from the broken edge of the arc that, presumably, marks the broken edge of the slab. The Sr-Pb-Nd isotope ratios of the slab-derived component in the breakup basalts most closely match those of the isotopically most depleted part of the Samoan seamount chain on the Pacific Plate that was adjacent to the site of breakup at 4–8 Ma, and differ from those of subsequent basalts in spreading segments of the surrounding backarc North Fiji and Lau Basins. Subduction of the Samoan Chain along the Vitiaz Trench Lineament may have controlled the limit of polarity reversal and, hence, where the double saloon doors (Martin, 2013) opened. Prior to breakup, Fijian volcanics were more similar isotopically to the Louisville Seamount Chain.

Plain Language Summary The subduction zone that included Tonga and Fiji was once connected to Vanuatu. We attribute the arc breakup to subduction of the Samoan Seamount Chain. Volcanism in Fiji accompanying breakup ranges from shoshonitic closest the tear in the arc, to low-K and boninitic farthest from it. The ambient mantle source of magma during breakup was the same as earlier in arc history but the slab-derived component changed during breakup. Post-breakup volcanism came from different mantle unaffected by subduction and derived from beneath the Pacific Plate.

Key Points:

- The breakup between Fiji and Vanuatu may have been triggered by subduction of Samoan seamounts
- Shoshonitic to low-K and boninitic volcanism accompanied breakup with increasing distance from the break
- The mantle source of later basalts in surrounding backarc basins and islands came from beneath the Pacific Plate north of the breakup site

Supporting Information:

Supporting Information may be found in the online version of this article.

Correspondence to:

J. Gill,
gillord@ucsc.edu

Citation:

Gill, J., Todd, E., Hoernle, K., Hauff, F., Price, A. A., & Jackson, M. G. (2022). Breaking up is hard to do: Magmatism during oceanic arc breakup, subduction reversal, and cessation. *Geochemistry, Geophysics, Geosystems*, *23*, e2022GC010663. https://doi.org/10.1029/2022GC010663

Received 15 AUG 2022
Accepted 5 OCT 2022
Corrected 21 DEC 2022

This article was corrected on 21 DEC 2022. See the end of the full text for details.

Author Contributions:

Conceptualization: James Gill, Allison Ann Price, Matthew G. Jackson
Data curation: James Gill
Formal analysis: Folkmar Hauff
Funding acquisition: Kaj Hoernle
Investigation: James Gill
Methodology: James Gill

1. Introduction

Most information about magma genesis in subduction zones is about their volcanic fronts under steady-state conditions (e.g., Gill, 1981; Plank, 2005; S. J. Turner & Langmuir, 2022). Non-steady-state events include subduction initiation (Ishizuka et al., 2018; Reagan et al., 2019), and interruptions of steady-states caused by episodes of flat-slab subduction or slab windows in continental arcs (Gutscher et al., 2000; Madson et al., 2006; Vogt, 1973), or back-arc basin opening in oceanic ones (Gill et al., 2021; Sdrolias et al., 2003). This paper deals with subduction cessation that most often accompanies collision of an arc with a continent or another arc such as in the Banda and Sangihe arcs in Indonesia, respectively (Elburg et al., 2005; Hanyu et al., 2012). The magmatic consequences of cessation can include quiescence, K-rich arc volcanism, and intra-plate-type volcanism.

This paper investigates an instance of subduction cessation in Fiji where, following a long period of normal subduction prior to 12 Ma, an oceanic arc broke across-strike rather than rifted along-strike, resulting in K-rich (shoshonitic) arc volcanism that was followed by intra-plate basalts, and the formation of new backarc basins as the arc fragments rotated apart and the influence of subduction ceased (Gill et al., 1984). We will show that (a) subduction of the older parts of the Samoan Seamount Chain contributed to magmatism where the arc broke, (b) melt from this subducted seamount track was restricted to within 100 km of the break and led to Au-Te ore deposits, and (c) the previous mantle wedge was rapidly replaced by new mantle unaffected by either subduction or a deep plume and might include the delaminated root of the Ontong Java Plateau.

2. Geological Context

2.1. The Upper Plate: Vitiaz Arc History

The once-continuous oceanic island arc on the easternmost Indian Plate above the subducting Pacific Plate in the southwest Pacific Ocean includes what are now the Vanuatu (New Hebrides) arc, Fiji, Tonga and Kermadec

Project Administration: James Gill, Folkmar Hauff
Resources: James Gill
Supervision: James Gill
Visualization: Erin Todd
Writing – original draft: James Gill
Writing – review & editing: James Gill, Erin Todd, Kaj Hoernle, Folkmar Hauff, Allison Ann Price, Matthew G. Jackson

arcs, and Lau-Colville Ridge remnant arc (Figure 1). This assembly is known collectively as the Vitiaz Arc (Gill & Gorton, 1973; Jezek et al., 1977; Packham, 1982), named for the Vitiaz Trench Lineament that stretches from the northern end of the Tonga Trench to the northern end of the Vanuatu Trench (Brocher, 1985; Pelletier & Auzende, 1996). Although that lineament is now a complex and poorly known transform fault boundary between the Pacific Plate and North Fiji Basin, the previously continuous arc was >3,000 km long and strongly arcuate with a decreasing angle of plate convergence to the northwest (Figure 2a). It was a mirror image of the modern Aleutian arc, but concave to the south instead of north.

The Vitiaz Arc is thought to have originated at about the same time as the Izu-Bonin-Mariana arc in the northwest Pacific (Hathway & Colley, 1994; Todd et al., 2012), and to have migrated eastward accompanying roll-back of

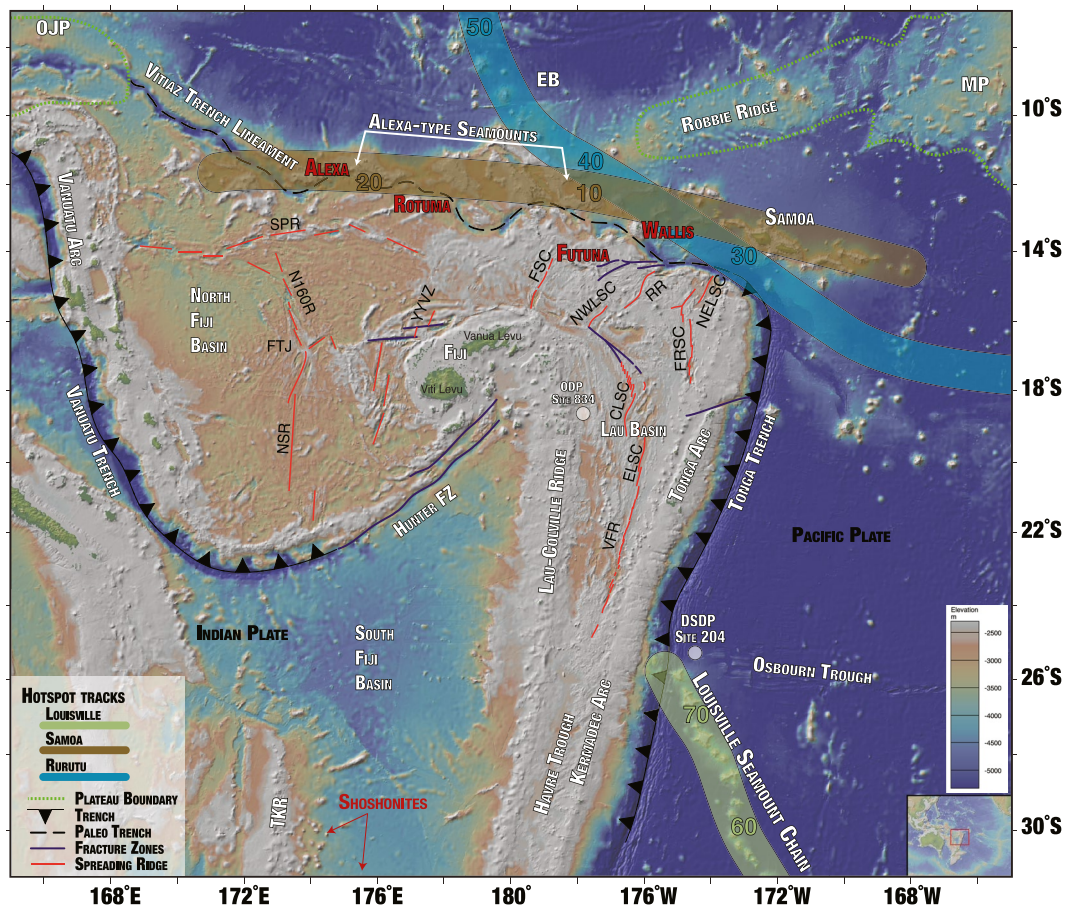

Figure 1. Tectonic features referred to in this paper. The spreading centers shown in orange are labeled as follows in clockwise fashion: NSR, North-South Ridge; FTJ, Fiji Triple Junction at 16°S; N160°R, North 160° Ridge; SPR, South Pandora Ridge; YYVZ, Yasawa-Yadua Volcanic Zone; FSC, Futuna Spreading Center; NWLSC, Northwest Lau Spreading Center; RR, Rochambeau Ridge; NELSC, Northeast Lau Spreading Center; FRSC, Fonualei Ridge Spreading Center; CLSC, Central Lau Spreading Center; ELSC, East Lau Spreading Center; VFR, Valu Fa Ridge. The location of most of these spreading centers is from Pelletier et al. (2001). NFB (North Fiji Basin) in later figures includes data from the NSR, FTJ, N160°R, and SPR. The LIP fragments outlined by green dashed lines are from B. Taylor (2006) as follows: OJP, Ontong Java Plateau; Robbie Ridge; and MP, Manihiki Plateau. The Louisville, Samoa, and Rurutu-Arago hot spot tracks and their ages shown in green, brown, and blue, respectively, are stylized after Jackson et al. (2020) using the Wessel and Kroenke (2008) absolute plate motion model anchored to the location of Vailulu'u seamount for the Samoan hotspot. Alexa Bank and the Rotuma, Futuna, and Wallis islands are young OIB-like volcanoes on both sides of the Vitiaz Trench Lineament (Hart et al., 2004; A. A. Price et al., 2017; R. C. Price et al., 1991; Sinton et al., 1985). The Alexa-type seamounts between the white arrows on the Pacific Plate include Alexa, Niulakita, Nukelaelae, Bustard, Bayonaise, and Tuscarora, from west to east. The Ellice Basin (EB) covers the entire northern part of the figure, both east and west of the Rurutu track (Benyshek et al., 2019). The South Fiji Basin shoshonites extend south of the figure and east of the Three Kings Rise (TKR; Mortimer et al., 2021). Data for pelagic and Louisville-derived volcaniclastic sediments from DSDP Site 204, and basalts from ODP Site 834 are shown in later figures. The bathymetry is from GeoMapApp.

the Tonga Trench during the 34–15 Ma opening of the South Fiji (backarc) Basin behind it that included the area now occupied by the North Fiji Basin (Herzer et al., 2011; Schellart et al., 2006). Vitiaz Arc volcanism resumed in the Middle to Late Miocene, products of which are known as the Lau Volcanic Group in the Lau Islands, Fiji (Cole et al., 1985; Gill, 1976; Woodhall, 1985a), the Wainimala Group in Viti Levu, Fiji (Gill, 1987; Hathway & Colley, 1994; Marien et al., 2022; Wharton et al., 1995), and the Western Belt of the Vanuatu arc (Carney et al., 1985). That configuration continued until the time considered by this paper (i.e., 12–3 Ma), and is shown in Figure 2a, after Martin (2013) and Schellart et al. (2006). Data for the Oligocene and Miocene arcs are shown in our figures.

At some time after 12 Ma, the Vitiaz Arc broke across-strike into a Vanuatu western portion and a Fiji-Tonga-Kermadec eastern portion, with Vanuatu rotating clockwise to its current position, Fiji rotating counterclockwise, and the North Fiji Basin opening between them. We will refer to this as "arc breakup" which differs from the more common arc rifting due to seafloor spreading between frontal and remnant arcs to form an intervening backarc basin. The breakup was first recognized by Chase (1971), Gill and Gorton (1973), and Packham (1973), and later supported by paleomagnetic studies in Vanuatu (Falvey, 1978; Musgrave & Firth, 1999) and Fiji (Malahoff, Hammond, Naughton, Keeling, & Richmond, 1982; G. K. Taylor et al., 2000), and by aeromagnetic anomalies in the North Fiji Basin (Malahoff, Feden, & Fleming, 1982). However, the age constraints from both the paleomagnetism and magnetic anomalies are uncertain. The most common interpretation is that arc breakup and rotation, and backarc spreading, started at ∼12 Ma (Auzende et al., 1995; Pelletier et al., 1993; Schellart et al., 2006).

Paired magnetic anomalies from seafloor spreading in the North Fiji and Lau Basins are as old as anomaly 2A (Gauss Chron; 2.6–3.6 Ma: Auzende et al., 1994; Zellmer & Taylor, 2001). However, all anomalies inferred to be older than that are from the low-resolution aeromagnetic mapping in the late 1970s. They are short and complex, and have not been confirmed by ship-borne magnetometers or detailed modeling of subchrons. None of them can be traced back to Anomaly 1. They reflect some combination of unstable creation of new oceanic crust (spreading), and attenuation of older crust plus extrusion and intrusion of younger magma (rifting). The latter characterizes the 125 km wide Havre Trough (Gill et al., 2021; Wysoczanski et al., 2010), and the western 80 km of the Lau Basin where the crust is about 50% thicker than in the eastern basin (Crawford et al., 2003). This makes the interpretation of magnetic anomalies as old as 12 Ma uncertain. Nevertheless, at least 100 km of the western North Fiji Basin must be older than 3.6 Ma which makes it likely that rifting and spreading there started by about 7 Ma if net extension is about 3 cm/y.

Paleomagnetic evidence for rotation older than 6 Ma comes only from altered hornblende andesite dikes on Tavua Island in the Mamanucu group west of Viti Levu, Fiji. Tilt and reversal tests for them are inconclusive, and their ∼10 Ma whole rock K-Ar age has not been replicated (G. K. Taylor et al., 2000). The mineralogy and bulk composition of the dikes (i.e., sample 71–391 in Gill, 1972) are more similar in composition to the high-K andesites of this study than to the Wainimala Group in adjacent Viti Levu shown as "Miocene" in our figures. Consequently, one can say with confidence only that Vanuatu and Fiji had started to separate by 6 Ma, after which Vanuatu rotated clockwise by at least 52°, and Fiji rotated counterclockwise by a similar amount. The result was called double-saloon-door tectonics by Martin (2013) whose reconstruction is shown in Figure 2.

Note, however, that there are important differences between the two broken arc segments in Figure 2. The Vanuatu segment reversed its subduction polarity, it is longer and adjacent to the Ontong Java Plateau, extension occurred behind the arc (i.e., no remnant arc is known) so that the entire previous volcanic arc rolled back along with the trench, and the extended region is wider and therefore may have started to open sooner. In contrast, the Fiji-Tonga segment maintained its subduction polarity, extension during trench roll-back was in the former forearc stranding its Miocene volcanic front on the remnant arc (Gill, 1976), and the oldest known backarc crust (4–5 Ma) at ODP Site 834 is within fragments of the remnant arc (Crawford et al., 2003; Cronan & Hodkinson, 1997).

Arc polarity reversal and the related eastward subduction beneath the Solomon Islands is attributed to its collision with the Ontong Java Plateau. The collision may have started with "soft-docking" of the plateau as early as 22 Ma in the southern Solomon Islands, but "hard-docking" is now thought to have begun at only ∼4 Ma (Mann & Taira, 2004). The aerial extent of the collision is uncertain. Mann and Taira (2004) speculate that the plateau extended as far east as Fiji such that subduction of its southern half reversed the polarity of Vanuatu at the same time as the Solomon Islands. That scenario is used in recent numerical models of the collision (Almeida et al., 2022; Wang et al., 2022). For several reasons, we prefer the more conventional alternative in which collision is restricted to the Solomon Islands. There is no evidence of accreted plateau in either Vanuatu or along the

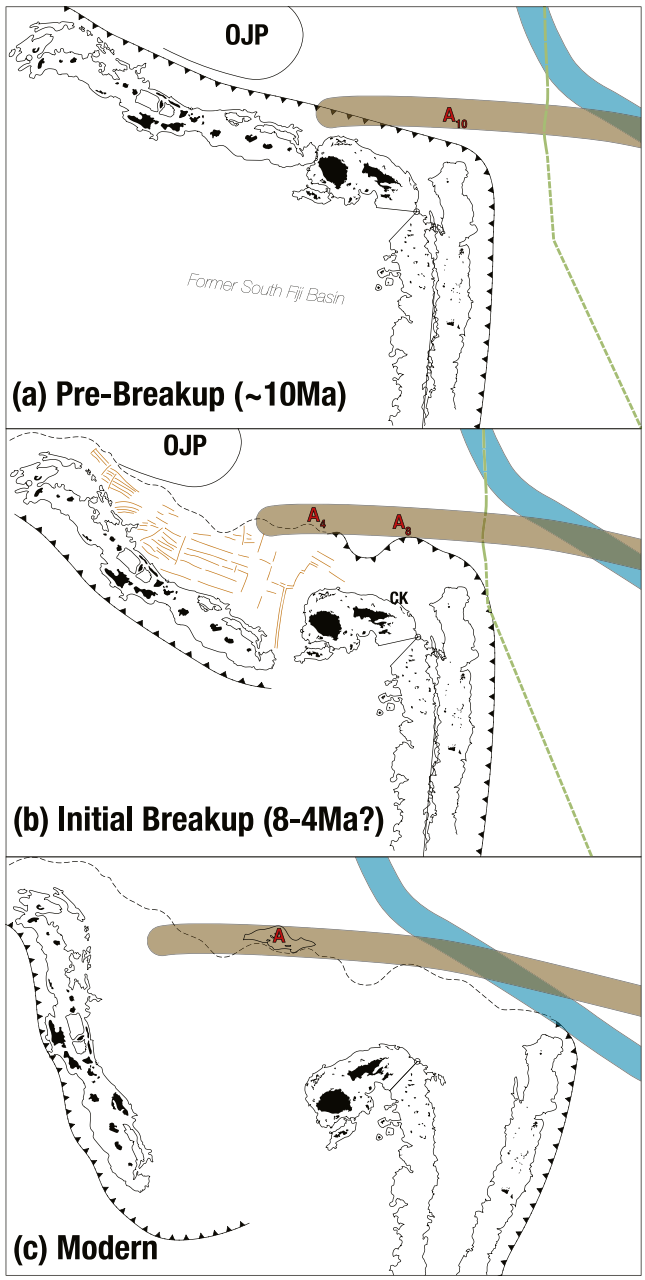

Figure 2. Schematic geologic history of the northern Vitiaz Arc and adjacent Pacific Plate. The position of the arc is based on Martin (2013) where (a) pre-breakup is his Figure 5, (b) initial breakup is his Figure 6 that incorporates 33° of counterclockwise of Fiji, and (c) summarizes our Figure 1. Martin assumed ages of 10–12 and 7.5 Ma, respectively, for panels (a and b), whereas we infer ages of ~10 and 4–8 Ma, respectively, for reasons given in the text. In both cases, the geometry post-dates opening of the South Fiji Basin. The southwest-dipping plate boundary in (a) schematically shows the location of the Vitiaz Trench ~100 km outboard of the 2,000 mbsl isobath that outlines the arc. The light brown lines north of the arc in (b) are from Martin (2013) and show magnetic lineations in the northwest North Fiji Basin that are interpreted as records of extension (rifting or spreading) west of the breakup site, with less to the east. CK in (b) shows the location of Cikobia Island near the pole of rotation for Fiji. Four features are shown on the Pacific Plate. OJP is the portion of the Ontong Java Plateau that appears in Figure 1; the feature continues to the northwest where it has collided with the Solomon arc (Mann & Taira, 2004). The brown and blue lines show the Samoan and Rurutu Hot Spot tracks, respectively, at ~10 and ~6 Ma, based on Buff et al. (2021), assuming a Pacific Plate motion azimuth of N64°W and velocity of 7 cm/y. The location of Alexa Bank (A) on the Samoan trace is shown for 4, 8, and 10 Ma. The scalloped shape of the Vitiaz Trench Lineament in (b) is the same as today (Figure 1) for simplicity. The green line shows the trace of the Louisville Seamount Chain based on Ruellan et al. (2003) and the Pacific Plate vector as above. Subsequently it subducts as the Lau Basin opens and would be south of panel (c) and under the Lau Ridge and Vanua Levu today.

Vitiaz Trench Lineament, nor of subducted plateau beneath the northwest North Fiji Basin. The eastern half of what Mann and Taira (2004; Figure 7) call the "now subducted edges of OJP" is where B. Taylor (2006) placed the Hikurangi portion of the former Ontong Java-Manihiki-Hikurangi mega-plateau. His reconstruction makes it unlikely that any part of the former mega-plateau would have intersected the Vitiaz Trench Lineament.

Another constraint on the timing of arc breakup is the presence of 7–12 Ma tonalitic plutons in Viti Levu, Fiji, that resulted from various combinations of crustal anatexis and differentiation of mantle-derived basalt (Gill & Stork, 1979; Marien et al., 2022). This time period was characterized by significant magmatic focusing, dilation, and deformation of the arc for several million years near where the break occurred because (a) both genetic processes require extensive intrusion of basalt into the crust, (b) the tonalites intrude broad anticlines and were rapidly uplifted, and (c) the crust of Viti Levu is thicker than in Vitiaz Arc segments further east (Chen et al., 2019). We suggest, therefore, that the start of organized spreading within the North Fiji Basin (i.e., the creation of paired magnetic anomalies in oceanic crust of normal thickness), and accompanying rotation of the arc segments, post-date the plutonism and occurred between magnetic anomalies 4 and 3 (8–5 Ma).

A final constraint on the timing of arc breakup is that the volcanism in Fiji discussed in this paper, and on Futuna Island to the northeast (Figure 1), remained arc-type until 3 Ma, and only then was it replaced by OIB-type volcanism (Gill & Whelan, 1989b; Grzesczyk et al., 1991; A. A. Price et al., 2017). The only arc-type volcanic rocks <3 Ma in Fiji are in Kadavu, just north of the eastern Hunter Fracture Zone (Figure 1). They are 0.4–2.9 Ma (Whelan et al., 1985) and adakitic, reflecting limited subduction of the young South Fiji Basin (Danyushevsky et al., 2008).

2.2. The Surrounding Backarc Basins

The clockwise rotation of Vanuatu and counter-clockwise rotation of Fiji opened the North Fiji Basin between them, just as the clockwise rotation of the Tonga arc opened the Lau Basin between it and Fiji. Concurrent extension also occurred, and continues, north and east of Fiji along several shorter segments (Pelletier et al., 2001; e.g., YYVZ in Figure 1). The detailed history of these segments is beyond the scope of this paper, but three aspects of their basalt geochemistry are important to it. First, there is evidence of a deep-seated plume source (i.e., high $^{3}He/^{4}He$ ratios) only along Rochambeau Ridge northeast of Fiji at 178°W (RR in Figure 1; Lupton et al., 2015). Although this is younger than, and well to the east of, the basalts discussed here, it raises the possibility of plume involvement in arc breakup (A. A. Price et al., 2017). Second, isotopic enrichments in OIB- and MORB-type basalts decrease southward away from the Vitiaz Trench Lineament, implying that their mantle sources came from beneath the Pacific Plate or Samoa as the plate boundary evolved from subduction to transform in character (Pearce et al., 2007; A. A. Price et al., 2017). The sub-Pacific Plate mantle may be filling a void left by an "avalanche" of the Vitiaz arc slab through the 600 km discontinuity (Pysklywec et al., 2003), or may just be drawn southward by opening of the adjacent backarc basins (e.g., Almeida et al., 2022). This new mantle replaced the former mantle wedge that underlay the Vitiaz Arc from Vanuatu to Kermadec since its inception. Ironically, the old mantle wedge under the eastern Indian Plate has been called isotopically "Pacific" for more than two decades because it is isotopically similar to what is now beneath the East Pacific Rise, whereas the new mantle that may come from beneath the Pacific Plate has been called isotopically "Indian" because the basalts have high $^{208}Pb/^{204}Pb$ at low $^{206}Pb/^{204}Pb$, and high $^{87}Sr/^{86}Sr$ and $^{176}Hf/^{177}Hf$ relative to $^{143}Nd/^{144}Nd$ ratios (Hergt & Hawkesworth, 1994; Pearce et al., 2007). We put "Indian" in quotation marks to stress that its use is solely to denote those geochemical traits rather than implying a genetic association with the mantle beneath Indian Ocean spreading centers. We will simply call it "new." Its $^{176}Hf/^{177}Hf$ isotope ratios reach 0.2835 in the YYVZ just north of Fiji (A. A. Price et al., 2014), one of the highest values in any MORB globally. This new mantle first appears ~3 Ma in the Lau Basin and Fiji (Gill & Whelan, 1989b; Hergt & Hawkesworth, 1994), but its age dependence elsewhere is unknown. If influx of a mantle plume, or this kind of new mantle, were the cause instead of consequence of breakup of the Vitiaz Arc, then it would leave distinctive geochemical markers in the rocks discussed in this paper.

ODP Site 834 in the rifted western Lau Basin (Figure 1) has special significance for this paper. It was drilled in a graben about 20 km east of the 2,000 mbsl isobath of the Lau Ridge, about 50 km east of the nearest Lau island, Moce. It reached 112 m into basalt that is isotopically "Pacific" but with slight backarc geochemical features (Hergt & Farley, 1994; Hergt & Hawkesworth, 1994; Hergt & Woodhead, 2007). The basalts underlie coarse volcaniclastic sediments from the Lau islands that were deposited during the Cochiti magnetic subchron of Anomaly 3 (4.2 Ma). Consequently, they are correlative with, but have much less of a subduction signature than, our breakup basalts nearby.

2.3. The Subducting Plate: Oceanic Plateaus, Seamount Chains, and the Melanesian Borderland

The Pacific Plate that subducted beneath the Vitiaz Arc throughout its history contains an abandoned spreading center known as the Osborn Trough that was once part of the boundary between the Pacific and Phoenix Plates (Figure 1; Billen & Stock, 2000). Spreading at the Osborn Trough, which is now near the boundary between the Tonga and Kermadec arcs, separated the Manihiki and Hikurangi portions of the once continuous Cretaceous Ontong Java-Manihiki-Hikurangi Plateau (OJMHP) Large Igneous Province (B. Taylor, 2006). Its formation and fragmentation had a lasting impact on the Vitiaz Arc in several ways. First, collision of two of the three large plateau fragments with subduction zones north and south of the Vitiaz Arc, caused subduction polarity reversal in the north (Ontong Java-Solomon Arc collision discussed above) and subduction cessation in the south (Hikurangi-Chatham Rise collision) prior to the more recent partial westward subduction of Hikurangi beneath North Island, New Zealand (Davy et al., 2008; Reyners et al., 2011). The southern edge of the Ontong Java plateau passed just a few hundred km north of the western Vitiaz Arc for tens of million years (Figure 1; Benyshek et al., 2019; B. Taylor, 2006). Slivers of it could have subducted beneath the Vitiaz Arc during that time much as slivers of the Hikurangi Plateau seem to have been subducted beneath the Kermadec Arc during the Miocene (Hoernle et al., 2021). "Plateau slivers" might just mean oceanic crust that is geochemically enriched or thickened by magmatism from plateau sources that contributed to loci of ridge spreading (e.g., Castillo et al., 2009).

The second impact is from the Louisville Seamount Chain (LSC) that is thought to be the tail of the OJMHP (Beier et al., 2011; Vanderkluysen et al., 2014). The western end of the LSC disappears into the Tonga-Kermadec Trench at 26°S which is the boundary between the actively spreading Lau Basin to the north and the still-rifting Havre Trough to the south (Figure 1; Ruellan et al., 2003). The age of this oblique collision of the LSC with the trench overlaps with, but is as uncertain as, when spreading started in the North Fiji and Lau basins. Whatever the exact timing, after the South Fiji Basin opened, the LSC lay within a few hundred km east of the Tonga-Fiji portion of the Vitiaz Arc throughout the Neogene (Figure 2). Because coarse volcaniclastic sediments from the LSC are found at DSDP Site 204 ~100 km north of it (Figure 1; S. Turner et al., 1997), LSC-derived sediment was available for subduction beneath Tonga and Fiji throughout the Neogene.

The final impact is not directly related to the OJMPH itself, but it is related to other plumes affecting the southwest Pacific Plate, namely the multiple seamount chains that passed near the Vitiaz Trench Lineament during the Neogene. They include the Macdonald, Rurutu-Arago, and Samoan seamount chains that sometimes are referred to as the "Hot Spot Highway" (e.g., Jackson et al., 2010). They form partly overlapping age-progressive seamount chains aligned along Pacific Plate flow lines (Figure 1). All of them except Macdonald passed just north of the Vitiaz Arc before or during the time when it broke into Vanuatu and Fijian segments. The Samoan chain in particular was within 100 km of the former trench (Hart et al., 2004), and may have been partially subducted during 20–3 Ma. None of the other hotspot tracks came this close to Fiji.

The westernmost, oldest-known seamounts of the Samoan chain are especially important for this paper. Following A. A. Price et al. (2022), we refer to them as Alexa-type; they are a subset of what was called WESAM by Hart et al. (2004). From west to east, the six for which geochemical data are published are Alexa, Niulakita, Nukulaelae, Bustard, Bayonaise, and Tuscarora. Their location is shown in general in Figure 1, and in detail by A. A. Price et al. (2022). Their basalts are more depleted isotopically than those farther east in the Samoan chain, having $^{87}Sr/^{86}Sr < 0.7044$, $^{143}Nd/^{144}Nd > 0.5128$, and $^{206}Pb/^{204}Pb < 19.05$.

Collectively, seamounts from the Samoan and Rurutu-Arago chains, and perhaps the northern portion of the LSC, and the Robbie Ridge protrusion from the Manihiki Plateau (Figure 1), festoon the southern margin of the Ellice Basin along what has been called the Melanesian Borderland immediately north of the Vitiaz Trench Lineament (Brocher, 1985). The borderland is a complex and highly faulted assortment of apparently old, well-sedimented volcanic seamounts, young volcanoes, and deep basins that form a zig-zag boundary that is reminiscent of where seamounts are subducting in trenches worldwide (Pelletier & Auzende, 1996). Some of the faulted seamounts are surrounded by extensive volcaniclastic aprons. Brocher (1985), Pelletier and Auzende (1996), and Schellert et al. (2006) all inferred that similar material has been subducted in the past west of Alexa Bank. Taken together, these materials include all geochemical types of ocean island basalts, although each chain is somewhat distinct geochemically (Jackson et al., 2010).

2.4. Summary of the Geological Context

All parts of the Vitiaz Arc have complex histories that are intertwined along the former arc's western trace that is called the Vitiaz Trench Lineament. Figure 2 illustrates that history and has three important implications for this paper. First, partial or complete subduction of one or more seamount chain, or slivers of the Ontong Java Plateau, might directly or indirectly have contributed to breakup of the Vitiaz Arc at ~180°E during the Late Miocene leading to rotation of Vanuatu, Fiji, and Tonga, and formation of the North Fiji and Lau Basins in their wake. At least the seamount chains were in the right place at the right time. Second, neither the history of the seamount chains and plateau slivers on the Pacific Plate, nor the history of backarc basin spreading and arc rotation on the Indian Plate, are known in sufficient detail to fix the time and cause of arc breakup precisely. However, breakup is likely to have started between 12 and 7 Ma. We favor the younger age for the start of spreading and significant rotation because it is the end of plutonism and uplift in Viti Levu, Fiji, that was adjacent to the tear in the arc. Third, abundant and diverse OIB materials (e.g., seamounts, plateau slivers, and volcaniclastic sediments) were available for subduction beneath the central portion of the Vitiaz Arc including Fiji throughout the last 15 million years after opening of the South Fiji Basin pushed the arc toward the path of the OJMPH and the Hot Spot Highway. This paper deals with the magmatic consequences of their interactions with the arc before and during breakup.

3. Samples, Lineaments, and Nomenclature

Tables 1 and 2 present new whole rock major and trace element, and Sr-Nd-Pb-Hf isotope ratios for 45 upper Miocene to Pliocene mafic volcanic rocks from throughout Fiji. Details about their location, rock type, and phenocryst mineralogy are included. Their general locations are shown in Figure 3. We selected the most mafic, representative, and dated samples from each island or volcanic center. These data are the first published comprehensive analyses for 14 of the islands, and for five of the volcanic centers on Viti Levu. Older XRF ± INAA data for some of the same samples are available along with data for another dozen samples from the same centers (Gill & Whelan, 1989a). Sr-Nd-Pb isotope data for four of the samples were published by Gill (1984) and happily agree with the new results within the older error. There are whole rock K-Ar ages for two-thirds of the samples (Whelan et al., 1985). Other comprehensive rock analyses have been published for the Sabeto, Tavua, and Namosi volcanoes on Viti Levu (Gill, 1970, 1987; Rogers & Settlefield, 1994; G.-Z. Sun et al., 2017), and for Tavua, Vatu-i-cake, and the Astrolabes (Leslie et al., 2009). Analyses of additional samples from these volcanoes, and from additional coeval volcanoes, are available in an Earth Chemistry Library (Gill, 2020). Hand specimens of most of the samples in this study, and other well-analyzed ones from the ECL, are archived in the US Smithsonian Museum of Natural History except for those with a 68-, 69-, or C prefix, for which agate-ground powders are available from the first author.

We group our samples into five geographic lineaments shown in Figure 3, the first three of which were identified by Gill and Whelan (1989a) and adopted by Leslie et al. (2009) and G.-Z. Sun et al. (2017): Viti Levu, Lomaiviti, Vatulele-Beqa, Vanua Levu, and Astrolabes (Table 1; Figure 3). The volcanic centers on these lineaments range in age from 5.2 to 3.0 Ma (Table 1; Whelan et al., 1985). We refer to them collectively as "breakup basalts."

We use the low-K, medium-K, high-K, and shoshonite categories of Gill (1981) to classify our samples in Tables 1 and 2. However, because most differences between our low- and medium-K samples are incidental for this paper, for simplicity we show them with the same symbol in figures and refer to them as medium-K in text. Most samples lie within their assigned category in a K_2O vs. SiO_2 diagram (Figure 4a), and most exceptions are the result of crystal accumulation in the shoshonitic absarokites, as can be inferred from a complementary K_2O vs. MgO diagram (Figure 4b) where the three groups are more clearly separated. The medium-K and high-K categories correspond roughly to the tholeiitic and calcalkaline ones used by Gill and Whelan (1989a). We avoided those terms because there is no consistent difference in Fe-enrichment between the categories for our samples.

The Viti Levu lineament consists of several large shoshonitic volcanoes that collectively constitute the Koroimavua and Mba stratigraphic Groups on the northern half of the island. We analyzed samples from the Sabeto, Nausori, and Tavua centers. They are flanked on the north by smaller coeval medium- and high-K edifices including Namosau, Vatia, Rakiraki, and Tova, from west to east. Tavua is the best studied of these volcanoes geologically, geochemically, and paleomagnetically (Gill, 1970; Ibbotson, 1967; Leslie et al., 2009; Malahoff, Hammond, et al., 1982; Rogers & Settlefield, 1994). Tavua and Sabeto host the large Emperor and Tuvatu epithermal Au-V-Te deposits, respectively (Spry & Scherbarth, 2006).

Geochemistry, Geophysics, Geosystems

10.1029/2022GC010663

Table 1
Whole Rock Analyses of Breakup Basalts

Sample	Type	Fig. 3 Legend	SiO_2	TiO_2	Al_2O_3	FeO^T	MnO	MgO	CaO	Na_2O	K_2O	P_2O_5	Li	Sc	V	Cr	Co
69-799	MK	Natewa	52.53	0.72	14.59	8.77	0.18	9.41	11.03	2.07	0.57	0.13	6.95	39.8	302	370	41.0
69-811	LK	Natewa	55.74	1.19	16.40	10.13	0.20	5.09	7.83	2.88	0.41	0.13	3.37	38.2	387	27.8	28.1
69-816	MK	Natewa	50.14	0.84	15.20	8.89	0.18	9.88	11.90	1.96	0.86	0.14	8.24	50.5	344	312	37.5
69-818	MK	Natewa	50.86	0.75	15.54	10.68	0.20	6.59	12.54	2.10	0.59	0.14	5.34	46.5	360	136	43.9
69-821	MK	Natewa	50.95	0.69	13.58	8.85	0.18	11.71	11.33	1.99	0.55	0.16	6.23	41.0	277	451	45.9
FJ73a	LK	Natewa	52.45	0.8	17.49	7.49	0.15	8.41	10.17	2.53	0.39	0.12		33	215	257	41
W107a	MK	Natewa	54.48	1.08	17.57	8.97	0.22	4.51	9.06	3.24	0.70	0.18	5.53	33.6	311	34.5	28.2
WQ17a*	LK	YD	53.68	0.78	16.88	8.53	0.18	6.12	10.96	2.18	0.54	0.17	7.55	41.7	352	70.8	30.4
WQ3a*	LK	Natewa	58.52	0.55	19.42	6.22	0.13	3.36	8.22	3.02	0.43	0.12	7.34	15.3	148	14.7	18.2
FJ56a	MK	Natewa	53.30	1.33	13.90	14.50	0.23	4.12	8.38	3.00	1.02	0.24		40	418	15	34
WQ13	LK	Natewa	52.75	0.76	16.03	9.55	0.18	6.22	11.27	2.59	0.5	0.16		37	304	110	51
W944	MK	NM	54.33	0.70	19.35	7.79	0.19	3.67	9.90	2.53	1.35	0.19	6.48	20.2	278	6.34	21.8
69-876	MK	NAM	55.42	0.82	18.05	8.02	0.13	4.26	8.36	3.42	1.26	0.23		29.5	256	27	21
WQ224	MK	MK	53.12	0.69	15.67	8.96	0.18	6.67	11.57	2.00	1.00	0.13	5.79	43.1	347	147	33.8
69-891	HK	V	52.94	0.81	19.81	7.29	0.15	4.40	10.18	2.71	1.46	0.25	13.2	34.1	357	16.0	21.4
W80	HK	R	49.29	0.82	17.77	9.56	0.18	6.97	11.11	2.41	1.61	0.27	8.59	31.8	341	151.0	36.3
W77	HK	T	49.95	0.99	18.16	10.32	0.21	5.35	11.06	2.47	1.24	0.24	7.12	35.7	355	30.4	35.7
W262	HK	NL	50.96	0.75	16.27	8.85	0.16	6.61	12.56	1.84	1.71	0.29	5.80	43.1	290	192	37.2
WQ220	HK	OV	49.20	1.00	18.69	10.09	0.21	5.60	11.24	2.42	1.31	0.24	8.37	30.8	301	17.3	28.6
69-840	HK	BT	49.27	0.88	14.48	9.89	0.20	8.65	12.91	2.11	1.37	0.23	8.32	45.5	338	222	41.8
W240	HK	BT	50.64	0.69	14.08	9.64	0.17	8.25	12.94	2.00	1.35	0.24	6.36	46.5	329	337	40.7
W245	HK	BT	50.42	0.85	15.67	9.73	0.20	6.61	12.34	2.32	1.62	0.25	6.35	39.3	371	146	34.9
C893	HK	MT	49.89	0.95	17.44	9.17	0.16	5.27	12.31	2.52	1.93	0.35	4.06	27.0	351	98	31.7
C880	HK	ML	49.59	0.78	13.04	10.26	0.19	11.13	11.39	1.77	1.58	0.28	6.67	41.9	302	389	49.1
WQ320	HK	B	55.65	0.68	17.10	8.00	0.16	4.09	8.45	3.84	1.76	0.27	11.5	26.6	265	26.3	25.2

Geochemistry, Geophysics, Geosystems

10.1029/2022GC010663

Table 1
Continued

Sample	Ni	Cu	Zn	Ga	Rb	Sr	Y	Zr	Nb	Cs	Ba
69-799	156	84.0	65.9	14.4	8.15	323	16.0	44.8	0.745	0.175	274
69-811	11.9	78.7	219	17.4	2.64	197	24.1	63.0	0.805	0.029	167
69-816	97.5	84.4	60.2	14.1	16.4	392	18.0	41.7	0.870	0.147	263
69-818	43.2	134	76.0	15.0	16.0	426	16.2	46.0	0.706	0.609	273
69-821	179	89.0	64.1	13.2	16.7	387	16.2	45.6	1.31	0.615	271
FJ73a	128				3.5	260	20.2	53	1.21	0.1	123
W107a	13.4	89.9	82.1	18.1	8.9	319	26.4	77.6	1.48	0.079	142
WQ17a*	28.8	111	72.9	16.0	9.87	367	22.1	44.3	0.683	0.244	228
WQ3a*	15.4	53.9	80.9	17.6	7.59	591	11.4	48.4	0.853	0.556	272
FJ56a	41				22.5	299	34.6	94.2	1.43	0.62	416
WQ13	30				12.6	315	19.1	39.7	0.77	0.54	171
W944	6.13	106	86.7	17.7	28.1	696	17.7	42	1.00	0.871	629
69-876	58	41.0	80	18.5	32.0	630	19.5	92.6	2.76	0.42	420
WQ224	31.4	156	75.7	14.6	16.2	338	16.1	34	1.2	0.659	557
69-891	12.9	114	65.9	17.4	23.9	814	21.7	40	1.05	0.549	431
W80	59.1	147	71.4	16.0	31.6	676	15.7	44	1.30	0.498	334
W77	21.5	109	74.7	16.8	22.6	574	17.8	49	1.40	0.233	483
W262	50.7	111	64.6	13.6	45.3	508	16.9	41	4.03	0.188	401
WQ220	18.4	54.8	64.1	14.4	21.3	609	16.2	39	0.950	0.579	524
69-840	42.6	139	76.1	15.0	23.7	480	16.6	42	1.57	0.294	532
W240	62.4	143	69.4	13.3	15.7	555	13.5	40	1.74	0.235	566
W245	30.9	169	152	15.6	26.7	586	17.5	51	3.73	1.68	821
C893	52.9	120	70.1	16.2	36.5	726	18.5	50	1.79	0.373	409
C880	159	185	73.4	13.2	32.5	448	16.4	39	1.31	0.183	356
WQ320	8.31	131	70.3	18.2	32.1	933	22.9	86	2.93	0.493	455

10.1029/2022GC010663

Table 1
Continued

Sample	Type	Fig. 3 Legend	La	Ce	Pr	Nd	Sm	Eu	Gd	Tb	Dy	Ho	Er	Tm	Yb	Lu	Hf
69-799	MK	Natewa	3.68	8.90	1.37	6.90	2.10	0.749	2.44	0.419	2.69	0.566	1.52	0.240	1.59	0.249	1.21
69-811	LK	Natewa	3.00	8.14	1.31	7.10	2.43	0.931	3.22	0.572	3.80	0.820	2.35	0.350	2.33	0.370	1.71
69-816	MK	Natewa	4.36	10.3	1.55	7.81	2.40	0.855	2.81	0.478	3.13	0.664	1.86	0.280	1.84	0.288	1.17
69-818	MK	Natewa	4.34	10.4	1.57	8.00	2.35	0.832	2.67	0.446	2.85	0.597	1.68	0.252	1.68	0.259	1.24
69-821	MK	Natewa	4.92	11.6	1.67	8.14	2.33	0.818	2.58	0.437	2.79	0.590	1.66	0.253	1.68	0.264	1.20
FJ73a	LK	Natewa	2.88	7.64	1.26	6.34	2.03	0.82	2.71	0.48	3.12	0.69	2	0.3	1.99	0.3	1.49
W107a	MK	Natewa	5.00	13.7	2.17	11.2	3.45	1.20	4.03	0.684	4.46	0.935	2.63	0.397	2.64	0.409	2.04
WQ17a*	LK	YD	5.13	11.0	1.86	9.55	2.77	0.975	3.29	0.538	3.49	0.744	2.07	0.310	2.04	0.323	1.24
WQ3a*	LK	Natewa	4.43	10.8	1.59	7.65	2.01	0.777									1.29
FJ56a	MK	Natewa	6.77	16.8	2.61	12.70	3.86	1.29	4.32	0.81	4.91	1.04	3.32	0.51	3.25	0.50	2.67
WQ13	LK	Natewa	4.15	9.84	1.62	7.94	2.36	0.88	2.98	0.49	3.02	0.65	1.85	0.27	1.79	0.27	1.25
W944	MK	NM	5.92	13.2	1.87	9.10	2.54	0.925	2.82	0.465	3.00	0.640	1.81	0.281	1.89	0.300	1.26
69-876	MK	NAM	11.3	23.7	3.28	13.7	3.18	1.07	3.27	0.5	2.94	0.59	1.86	0.28	1.78	0.28	2.44
WQ224	MK	MK	3.58	8.2	1.23	6.29	1.95	0.712	2.39	0.417	2.73	0.583	1.65	0.254	1.67	0.263	1.06
69-891	HK	V	5.80	12.6	1.87	9.38	2.82	1.00	3.33	0.560	3.62	0.763	2.18	0.334	2.24	0.355	1.26
W80	HK	R	7.76	17.2	2.35	11.0	2.87	1.00	2.96	0.461	2.82	0.574	1.59	0.239	1.55	0.240	1.25
W77	HK	T	6.33	14.2	2.01	9.76	2.70	1.01	3.03	0.491	3.09	0.634	1.76	0.267	1.77	0.274	1.37
W262	HK	NL	7.55	15.5	2.13	9.79	2.55	0.903	2.83	0.456	2.85	0.599	1.67	0.251	1.66	0.264	1.14
WQ220	HK	OV	4.75	10.3	1.67	8.36	2.39	0.908	2.70	0.439	2.80	0.581	1.62	0.241	1.59	0.249	0.945
69-840	HK	BT	6.39	14.3	2.16	10.5	2.90	0.989	3.10	0.482	2.95	0.591	1.53	0.239	1.53	0.238	1.34
W240	HK	BT	7.11	15.6	2.19	10.3	2.58	0.861	2.62	0.405	2.44	0.495	1.36	0.202	1.33	0.207	1.13
W245	HK	BT	8.19	17.9	2.46	11.4	2.87	0.952	3.05	0.490	3.04	0.629	1.76	0.262	1.74	0.271	1.39
C893	HK	MT	6.38	14.6	2.13	10.4	2.90	1.02	3.22	0.523	3.27	0.676	1.87	0.278	1.84	0.286	1.46
C880	HK	ML	5.67	12.7	1.91	9.28	2.66	0.924	2.94	0.468	2.91	0.591	1.56	0.242	1.59	0.249	1.23
WQ320	HK	B	17.3	36.2	4.78	20.9	4.66	1.36	4.35	0.633	3.73	0.768	2.17	0.322	2.13	0.342	2.16

Geochemistry, Geophysics, Geosystems

10.1029/2022GC010663

Table 1
Continued

Sample	Ta	Pb	Th	U	$^{87}Sr/^{86}Sr$	$^{143}Nd/^{144}Nd$	$^{176}Hf/^{177}Hf$	$^{206}Pb/^{204}Pb$	$^{207}Pb/^{204}Pb$	$^{208}Pb/^{204}Pb$
69-799	0.051	1.87	0.418	0.211	0.703649	0.513016		18.9352	15.5737	38.6745
69-811	0.064	1.94	0.348	0.193	0.703563	0.513061	0.283158	18.8046	15.5531	38.4011
69-816	0.059	1.61	0.532	0.237						
69-818	0.051	2.33	0.527	0.294	0.703758	0.512998		18.9013	15.5674	38.6048
69-821	0.083	2.21	0.618	0.257	0.703597	0.513020		18.9873	15.5782	38.6744
FJ73a		1.35	0.24	0.11						
W107a	0.104	1.52	0.388	0.217	0.703342	0.513041	0.283151	18.7141	15.5509	38.3178
WQ17a*	0.052	1.71	0.382	0.211	0.703619	0.513023		18.8185	15.5640	38.4883
WQ3a*	0.064	1.89	0.253	0.106	0.703456	0.513034		18.8397	15.5655	38.5429
FJ56a	0.06	4.28	0.76	0.38	0.703760	0.513046	0.283160	18.917	15.566	38.622
WQ13		1.84	0.38	0.2	0.70361					
W944	0.059	4.87	0.894	0.388	0.703630	0.513016	0.283159	18.9548	15.5708	38.7104
69-876	0.11	5.76	1.64	0.61	0.703752	0.512993	0.2832	18.83	15.554	38.534
WQ224	0.079	2.43	0.354	0.209	0.704278	0.513002		18.7978	15.5754	38.6319
69-891	0.060	5.06	0.670	0.276						
W80	0.079	3.83	1.08	0.415	0.703766	0.512976	0.283136	18.9476	15.5746	38.7105
W77	0.092	1.83	0.641	0.309	0.703830	0.513021		18.8955	15.5718	38.6822
W262	0.216	2.80	0.768	0.284	0.703961	0.512896	0.283094	18.8204	15.5843	38.7342
WQ220	0.061	3.27	0.416	0.188	0.703894	0.513003		18.8939	15.5767	38.7034
69-840	0.099	2.96	0.634	0.315						
W240	0.099	3.59	0.704	0.317						
W245	0.202	2.92	0.754	0.334	0.704548	0.512926		18.8157	15.5755	38.6595
C893	0.114	4.79	0.600	0.288	0.703774	0.513000		18.7154	15.5742	38.6170
C880	0.083	2.82	0.517	0.253	0.703744	0.512953	0.283166	18.6931	15.5716	38.5709
WQ320	0.166	4.64	1.86	0.841				18.850	15.550	38.490

Note. See Table 2 for continuation and Tables S1 and S2 for more complete information.

Geochemistry, Geophysics, Geosystems

10.1029/2022GC010663

Table 2
Whole Rock Analyses Continued

Sample	Type	Fig. 3 Legend	SiO_2	TiO_2	Al_2O_3	FeO^T	MnO	MgO	CaO	Na_2O	K_2O	P_2O_5	Li	Sc	V	Cr	Co
68-64	SH	S	52.35	0.65	20.32	7.19	0.15	3.69	9.19	2.78	3.22	0.46	11.6	17.5	260	42.1	22.1
W10	SH	S	52.72	0.68	18.92	7.27	0.19	3.81	8.14	4.27	3.62	0.38	12.9	18.1	334	7.24	21.5
69-865	SH	NS	50.51	0.72	15.34	9.58	0.21	5.26	11.96	2.83	2.81	0.78	16.7	30.1	420	26.6	29.7
W5	SH	NS	52.03	0.71	19.57	8.14	0.16	4.30	8.11	2.82	3.64	0.53	12.1	17.8	281	44.6	25.3
69-895	SH	TV	49.57	0.59	12.59	9.88	0.19	10.57	12.36	2.00	1.94	0.31	11.7	47.0	309	393	45.4
68-897	SH	TV	49.99	0.76	16.75	9.65	0.24	5.87	10.03	2.24	3.77	0.7		32	322	45	38
W68	SH	TV	50.61	0.61	12.39	10.02	0.18	10.14	11.90	1.79	2.06	0.31	10.5	42.5	293	388	46.0
WQ233	SH	VC	49.23	0.76	14.6	9.09	0.16	8.97	9.87	3.11	2.61	0.58		30	315	567	50
WQ223a	SH	W	48.8	0.67	12.96	9.53	0.17	11.88	8.97	1.9	3.43	0.58		16	246	916	54
W286	SH	G	51.62	0.65	11.91	9.74	0.20	9.15	12.27	1.62	2.56	0.28	14.3	47.7	338	268	38.1
W301	SH	VL	48.96	1.42	17.83	9.23	0.22	4.06	10.03	3.19	4.38	0.68	20.5	15.2	353	9.08	26.6
W310	SH	VL	50.82	1.17	19.22	6.61	0.17	2.63	7.70	6.44	4.70	0.54	50.9	9.80	256	5.29	17.9
WQ311	SH	YN	54.50	0.64	15.61	8.26	0.14	4.68	8.91	2.87	3.95	0.42	14.4	32.1	293	94.5	27.0
WQ317	SH	U	52.22	0.67	14.41	9.90	0.18	6.11	10.61	2.50	2.95	0.46	8.86	41.9	347	154	36.2
WQ328	SH	A	51.57	1.11	17.82	9.12	0.24	4.48	8.72	3.1	3.33	0.51	22.1	12	233	16	29
WQ329	SH	A	51.04	0.86	15.32	10.25	0.19	5.82	10.81	3	2.41	0.3	23	28	299	73	29
AK1	BON	CK	56.66	0.21	15.68	6.88	0.11	7.5	8.9	2.69	0.49	0.1	5.6	38		335	
C48 glass	BON	CK	58.02	0.23	16.27	6.96	0.11	5.83	8.43	2.82	0.59	0.03	5.3	36		186	
C1 glass	LK	CK	54.80	1.00	16.33	8.14	0.17	6.04	10.32	2.86	0.22	0.11	5.27	34	262	165	29.0
C2 glass	LK	CK	54.91	1.00	16.32	8.15	0.15	5.99	10.29	2.88	0.22	0.10	5.27	34	263	162	29.1

Geochemistry, Geophysics, Geosystems

10.1029/2022GC010663

Table 2
Continued

Sample	Ni	Cu	Zn	Ga	Rb	Sr	Y	Zr	Nb	Cs	Ba
68-64	13.8	223	66.5	15.6	56.6	1370	14.2	49.0	0.906	0.781	709
W10	6.48	242	73.6	17.2	57.1	999	19.1	51.9	1.14	0.755	647
69-865	18.7	125	79.9	12.4	51.3	1227	23.8	123	1.68	7.20	788
W5	15.5	245	77.9	16.0	82.8	1125	16.5	61.7	1.10	1.41	686
69-895	94.0	126	73.8	12.2	57.2	1452	14.1	33.8	0.665	1.38	490
68-897	22				72.0	1370	26.0	45.0			968
W68	102	127	76.0	12.7	37.8	841	14.4	35.2	0.652	0.458	455
WQ233	250				49	1138	16.8	57.7	1.94	1.7	430
WQ223a	355				44	1228	13.1	59.8	1.63	0.47	431
W286	48.0	185	68.6	12.5	58.2	1044	12.9	33.3	2.02	0.400	519
W301	11.8	491	118	19.4	63.9	2654	26.6	151	16.4	1.52	891
W310	4.10	159	91.3	22.5	73.5	2825	23.3	215	22.7	1.53	911
WQ311	17.6	126	64.2	14.3	74.8	1136	16.2	59.3	4.27	0.553	596
WQ317	24.2	231	74.9	15.1	60.5	1097	19.1	79.1	1.81	0.424	471
WQ328	9				33	849	15.8	65	6.7	1.3	384
WQ329	79				54	853	13.6	51.2	2.8	1.16	346
AK1	290				15	83	7	21	0.62	0.52	108
C48 glass	66				14	122	9	31		0.38	102
C1 glass	48.1	49.4	79.8	16.3	3.33	160	19.8	72	1.13	0.08	33
C2 glass	47.3	53.7	78.8	16.4	3.27	159	20.2	73	1.13	0.07	32

Geochemistry, Geophysics, Geosystems

10.1029/2022GC010663

Table 2
Continued

Sample	Type	Fig. 3 Legend	La	Ce	Pr	Nd	Sm	Eu	Gd	Tb	Dy	Ho	Er	Tm	Yb	Lu	Hf
68-64	SH	S	7.06	14.9	2.03	9.47	2.44	0.864	2.51	0.397	2.43	0.507	1.43	0.217	1.46	0.232	1.22
W10	SH	S	11.4	23.3	3.12	14.3	3.59	1.18	3.58	0.549	3.30	0.670	1.87	0.283	1.86	0.294	1.44
69-865	SH	NS	21.2	48.1	6.89	33.1	8.32	2.44	6.96	0.880	4.53	0.833	2.19	0.313	2.02	0.313	2.61
W5	SH	NS	8.06	17.5	2.35	10.9	2.78	0.941	2.84	0.447	2.75	0.573	1.61	0.246	1.66	0.264	1.49
69-895	SH	TV	5.67	12.7	1.83	8.99	2.54	0.855	2.68	0.413	2.51	0.513	1.43	0.213	1.41	0.222	0.941
68-897	SH	TV	13.5	22.6	3.9	20	4.9	1.4	4.9	0.75		0.79	1.9		1.9		1.2
W68	SH	TV	5.88	12.8	1.87	9.17	2.59	0.875	2.76	0.419	2.56	0.515	1.34	0.214	1.39	0.217	1.02
WQ233	SH	VC	11.5	24.1	3.33	14.5	3.73	1.21	3.44	0.52	2.69	0.53	1.53	0.23	1.41	0.22	1.54
WQ223a	SH	W	12.6	27.3	3.61	15.8	3.85	1.24	3.46	0.47	2.4	0.44	1.26	0.18	1.08	0.18	1.62
W286	SH	G	6.36	13.2	1.79	8.41	2.24	0.748	2.40	0.372	2.27	0.461	1.27	0.192	1.26	0.197	0.961
W301	SH	VL	31.8	69.5	8.32	34.3	6.80	2.11	6.06	0.862	4.86	0.942	2.54	0.365	2.37	0.362	3.37
W310	SH	VL	36.8	77.9	8.91	35.3	6.72	2.02	5.59	0.778	4.26	0.819	2.25	0.325	2.15	0.325	4.09
WQ311	SH	YN	11.9	24.8	3.31	14.6	3.34	1.03	3.24	0.475	2.76	0.559	1.55	0.238	1.60	0.254	1.52
WQ317	SH	U	17.4	39.8	5.73	26.6	6.13	1.70	5.28	0.691	3.57	0.662	1.74	0.247	1.59	0.246	1.85
WQ328	SH	A	8.95	19.4	2.61	11	2.57	0.74	2.4	0.24	2.18	0.47	1.31	0.2	1.22	0.18	1.3
WQ329	SH	A	6.9	14.8	2.17	9.51	2.37	0.71	2.24	0.44	2.24	0.42	1.52	0.24	1.38	0.23	1.35
AK1	BON	CK	0.68	1.28	0.19	0.78	0.31	0.133	0.66	0.145	1.23	0.28	1.01	0.153	1.17	0.197	0.75
C48 glass	BON	CK	1.01	1.92	0.34	1.61	0.69	0.24	0.98	0.21	1.54	0.36	1.14	0.179	1.45	0.231	1.03
C1 glass	LK	CK	3.15	9.38	1.49	7.68	2.34	0.88	2.96	0.53	3.45	0.72	2.20	0.32	2.26	0.319	1.81
C2 glass	LK	CK	3.10	9.31	1.49	7.55	2.39	0.87	2.95	0.51	3.41	0.73	2.20	0.32	2.23	0.321	1.83

Geochemistry, Geophysics, Geosystems

10.1029/2022GC010663

Table 2
Continued

Sample	Type	Fig. 3 Legend	Ta	Pb	Th	U	$^{87}Sr/^{86}Sr$	$^{143}Nd/^{144}Nd$	$^{176}Hf/^{177}Hf$	$^{206}Pb/^{204}Pb$	$^{207}Pb/^{204}Pb$	$^{208}Pb/^{204}Pb$
68-64	SH	S	0.059	6.32	0.841	0.493	0.703756	0.513005	0.283155	18.9906	15.5651	38.6647
W10	SH	S	0.068	5.55	1.77	1.04	0.703912	0.512998	0.283147	18.9815	15.5688	38.6598
69-865	SH	NS	0.085	8.65	2.52	1.69						
W5	SH	NS	0.071	6.52	0.954	0.566						
69-895	SH	TV	0.041	5.50	0.658	0.304	0.703866	0.512999	0.283165	18.9600	15.5660	38.6910
68-897	SH	TV		11	1.7	0.68						
W68	SH	TV	0.043	5.98	0.699	0.200	0.703860	0.513007		18.9625	15.5718	38.7037
WQ233	SH	VC	0.14	6.4	1.55	0.68	0.703768	0.512988	0.283140	18.9820	15.5760	38.7000
WQ223a	SH	W	0.07	8.7	1.48	0.78	0.704069	0.513006	0.283165	18.9930	15.5730	38.6830
W286	SH	G	0.117	5.02	0.583	0.295	0.704240	0.512952		18.8558	15.5780	38.7458
W301	SH	VL	0.960	10.2	3.28	1.05	0.703640	0.512887	0.283067	18.8435	15.5651	38.6050
W310	SH	VL	1.231	15.2	5.12	1.70	0.703637	0.512914	0.283069	18.8529	15.5668	38.6158
WQ311	SH	YN	0.246	4.71	1.36	0.523	0.703606	0.512944		18.8995	15.5730	38.6459
WQ317	SH	U	0.094	5.22	1.53	0.676	0.703468	0.513026		18.7876	15.5443	38.3947
WQ328	SH	A		5.7	0.96	0.31						
WQ329	SH	A		5.5	0.8	0.27	0.704230					
AK1	BON	CK	0.06	1.22	0.103	0.047	0.704487	0.512932		18.8069	15.5843	38.5485
C48 glass	BON	CK		1.79	0.158	0.094	0.704348	0.512940	0.283081	18.8036	15.5741	38.5305
C1 glass	LK	CK	0.078	0.803	0.175	0.078	0.702995	0.513068		18.6086	15.5276	38.2317
C2 glass	LK	CK	0.073	0.798	0.180	0.077	0.703009	0.513071	0.283148	18.6048	15.5244	38.2224

Note. See Tables S1 and S2 for more complete information.

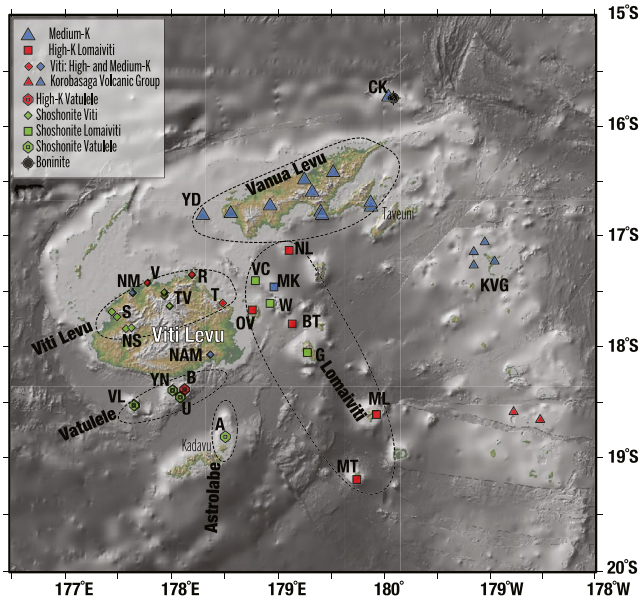

Figure 3. Location of samples and lineaments. The abbreviations identify islands or volcanic centers as follows: A, Astrolabe; B, Beqa; BT, Batiki; CK, Cikobia; G, Gau; KVG, Korobasaga Volcanic Group (Lau); MK, Makogai; ML, Moala; MT, Matuku; NAM, Namosi; NL, Namenalala; NM, Namosau; NS, Nausori; OV, Ovalau; R, Rakiraki; S, Sabeto; T, Tova; TV, Tavua; U, Ugaga; V, Vatia; VC, Vatu-i-cake; VL, Vatulele; W, Wakaya; YD, Yadua; and YN, Yanuca. The symbols are explained in the legend and are used in all figures. The triangles in Vanua Levu show sample sites in the Natewa Formation. The four small blue (medium-K) KVG triangles in northern Lau are Vanua Balavu, Kibobo, Malima, and Kanacea islands. The two small red (high-K) KVG triangles between 18° and 19°S are Olorua and Moce islands. ODP Site 834 lies just east of the figure at 18.57°S. Bathymetry as in Figure 1.

The Lomaiviti lineament lies south of Vanua Levu between Viti Levu and the Lau Ridge, in the armpit apex of Fiji's counterclockwise rotation (Figures 1 and 3). The edifices are mostly shoshonitic and high-K volcanoes that are 3–4 Ma in age and rise from ambient seafloor 2,000–3,000 mbsl, deepening southward (Coulson, 1976). Samples from one of them, Vatu-i-cake, were studied by Leslie et al. (2009). Our samples are from subaerial lava flows, or clasts from volcanic breccias, on nine of the islands.

The Vatulele-Beqa lineament lies 15–40 km south of Viti Levu, and includes Vatulele and the small islets of Yaunca and Ugaga within the reef surrounding Beqa. All are shoshonitic except Beqa that is high-K. They are 4–5 Ma as are the Viti Levu shoshonites. Several younger 3–4 Ma shoshonites centers lie 50 km southeast of Beqa in the Astrolabe Reef near Kadavu (Leslie et al., 2009).

Our samples from Vanua Levu, Fiji's second largest island, are from the basaltic Natewa Group that constitutes most of the island. Some are from named formations within the Group (Table S1) that may represent separate volcanic centers (Coulson, 1971; Rickard, 1966). They are distributed ~150 km east-west and ~40 km north-south, are from lava flows, dikes, and clasts in volcanic breccias, and are geochemically representative of the ~100 samples for which we have unpublished major element analyses. The Natewa Group formed a shallow submarine to subaerial ridge and includes pillow basalts that are now up to 1,000 m above sea level. Most are low-to medium-K, and similar in composition to the coeval Korobasaga Volcanic Group in the northern Lau islands (small blue triangles in Figure 3: Cole et al., 1985; Gill, 1976; Hergt & Woodhead, 2007). Korobasaga samples from the southern Lau islands of Moce and Olorua are slightly high-K, as are one sample each from Kibobo and Kanacea islands. We interpret the Lau islands and Vanua Levu as the Pliocene volcanic front of the Fiji-Tonga portion of the Vitiaz Arc, so that all breakup basalts are part of a stranded remnant arc.

We include one sample (69–876) from the older Namosi Andesite formation in southeast Viti Levu that was a volcano that reached sea level at ~6 Ma and hosts an economic porphyry copper ore body (Orovan et al., 2018; Tanaka et al., 2010). Although this sample also is medium-K, it is richer in K and other incompatible elements than those from Vanua Levu, befitting its more rearc location. This formation was the source of a prototypical calcalkaline andesite (S. R. Taylor et al., 1967) that was the first known to have an eclogite liquidus mineralogy at 3 GPa and, therefore, to be a potentially primary slab melt (Green & Ringwood, 1968). Geological and mineralogical information about the formation is provided by Gill (1987).

The last center is Cikobia, a 2 × 10 km island that lies 60 km north of the northeast tip of Vanua Levu (Figure 1; Woodhall, 1985b). We include data for it because its volcanic rocks are distinctive, and it is relatively inaccessible. If Lomaiviti is the armpit of the Lau Ridge, then Cikobia is its protruding elbow on the edge of the Lau Basin near one end of the Futuna Spreading Center. Its pre-rotation location at ~14°S (Figure 2) places it near the site of the boninites at the north end of the Tonga Ridge. Although Cikobia is mostly covered by limestone, its underlying volcanic rocks crop out for ~2 km on the southeast coast. D.Woodhall mapped the island and provided samples C48 from near Oneva and AK1 from near Qaraibo. Gill later collected C1 and 2 in the same general area. All are pillow lavas and breccias, and the latter have cm-thick glass rims. The overlying limestone contains N17 foraminifera (Late Miocene). A K-Ar whole rock total fusion age of the crystalline pillow interior of C48 was determined by R. Duncan in February 1985 as follows: 7.39 ± 0.20 Ma; $K = 0.481$ wt.%; Rad.^{40}Ar = 0.5428 10^{-6} mol/gm; %Rad.^{40}Ar = 29.07. C48 and AK1 are low-Ti (0.25 wt.% TiO_2), boninitic high-Mg andesites (whole rock 57% SiO_2; 7.5% MgO; Mg# 66). They are chemically most similar to the North Tonga boninites in Dredge 113 of Falloon et al. (2008) that are accompanied by 2.7 Ma adakitic rhyolite. In contrast, C1 and 2 are similar to the low-K basalts in Vanua Levu. They have a few percent of plagioclase (An87) and clinopyroxene (Mg#86 with 0.8% Cr_2O_3) mantled by orthopyroxene (Mg#86–82) micro-phenocrysts in vesicular glass. Woodhall's (1985b) map unit was described, with the benefit of

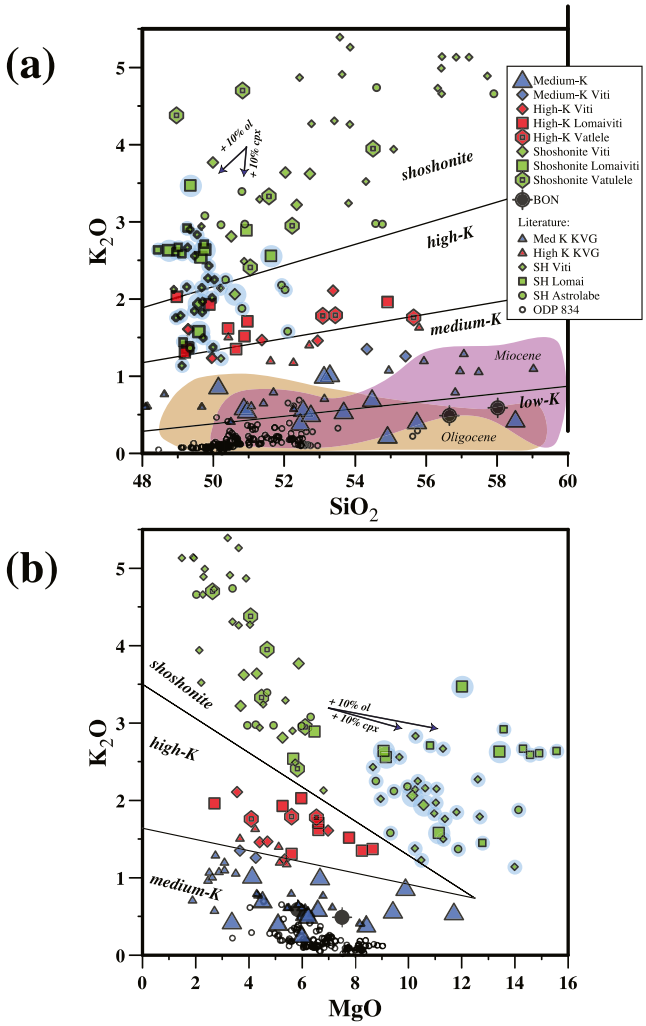

Figure 4. (a) SiO_2 vs. K_2O; (b) MgO vs. K_2O. Symbols are as in Figure 3. The larger symbols show data from Table 1. The smaller symbols show data from the literature: shoshonites from Leslie et al. (2009), Rogers and Settlefield (1994), and G.-Z. Sun et al. (2017); and the 3–5 Ma Korobasaga Volcanic Group (KVG) in the Lau islands from Cole et al. (1985) and Gill (1976). ODP Site 834 data are from Hergt and Farley (1994). The field for Miocene includes the Lau Volcanic Group (Cole et al., 1985; Gill, 1976), and the Wainimala Group of Viti Levu (Todd et al., 2021). The field for Oligocene includes the Yavuna Group of Viti Levu (Todd et al., 2012, 2021). The legend suffix (e.g., Viti) denotes the lineament shown in Figure 3. The boundaries for low, medium, and high-K, and shoshonite are from Gill (1981). The highlighted samples are absarokites that have accumulated cpx > ol. The effect of accumulating 10% of each mineral are shown by the arrows. The boundaries in (b) are specific to this study.

our analyses of AK1 and C48, as "Basalt, basaltic andesite and andesite (aff. boninite) pillow lava, hyaloclastite and interbedded sediments near top"; his accompanying report is unpublished.

The Vanua Levu, Viti Levu, and Vatulele-Beqa lineaments are northeast-trending, subparallel to the current trend of the Fiji Platform and orthogonal to its torn edge facing the North Fiji Basin (Figure 3). We speculate that they and the Lomaiviti lineament are stress fractures from rupturing and rotation of the arc.

Younger intra-plate Fijian ocean island basalts (FOIB) occur in Lomaiviti, Vanua Levu, Taveuni, and some of the Lau islands. Analyses and discussion of them are given by Gill and Whelan (1989b) and A. A. Price et al. (2017), and we show data for them in figures.

4. Analytical Methods

All samples are fresh subaerial whole rocks. Visible alteration was removed before crushing. For elemental analyses, they were broken in a steel jaw crusher and pulverized in agate. For isotope analyses, separate rock chips were leached in 2.5 N HCl at 70°C for an hour before dissolution.

Table S1 includes the sources of the data. Most were obtained in Kiel during 2018–2020 following the methods in Hauff et al. (2021), namely major elements by XRF, trace elements by solution ICPMS and XRF, Sr and Nd isotopes by TIMS, Pb isotopes by double-spiked TIMS, and Hf isotopes by MC-ICPMS. The major and trace elements in the C1, 2 Cikobia glass samples were analyzed in Kiel by microprobe and LA-ICPMS, respectively. See Hauff et al. (2021) for analytical details and results for standards.

Five of the samples were analyzed earlier following methods in Pearce et al. (2007), and eight were analyzed earlier at UCSC following methods in Ryder et al. (2006). Trace elements in the two Cikobia boninites were analyzed at Memorial University Newfoundland following methods of Jenner et al. (1990). The principal difference from the Kiel methods is that Pb isotope measurements in these cases were by Tl-addition MC-ICPMS. The UCSC samples were pulverized in WC and therefore no Ta concentrations are reported for them, and their Nb contents may be up to 0.5 ppm too high. These are the first Pb isotopes using a spiked technique, and the first Hf isotopes, for any breakup basalts. Tables 1 and 2 contain the new analytical results. Tables S1 and S2 provide a more complete version of that table that includes sample locations, geological context, age, analytical errors for isotope ratios, petrography, and results for standards.

5. Results

5.1. Phenocryst Mineralogy

All samples are variably porphyritic; although no groundmass is pure glass, the Cikobia samples were hand-picked to be mostly glass. Some mineral modes are included in Table S1. The phenocrysts of the medium-K and high-K rocks are plagioclase followed in abundance by clinopyroxene, olivine, and magnetite. Some medium-K samples have orthopyroxene, and some high-K ones have hornblende. The abundance of clinopyroxene relative to MgO is greater in the high-K than medium-K samples. The shoshonitic series includes absarokites that have clinopyroxene and olivine but not plagioclase, vs. shoshonites with all three ± biotite, leucite, nepheline, and analcime in coarse-grained varieties called monzonite (Rodda, 1976). The absarokites often have >50% phenocrysts, with about four times more clinopyroxene than olivine. Leslie

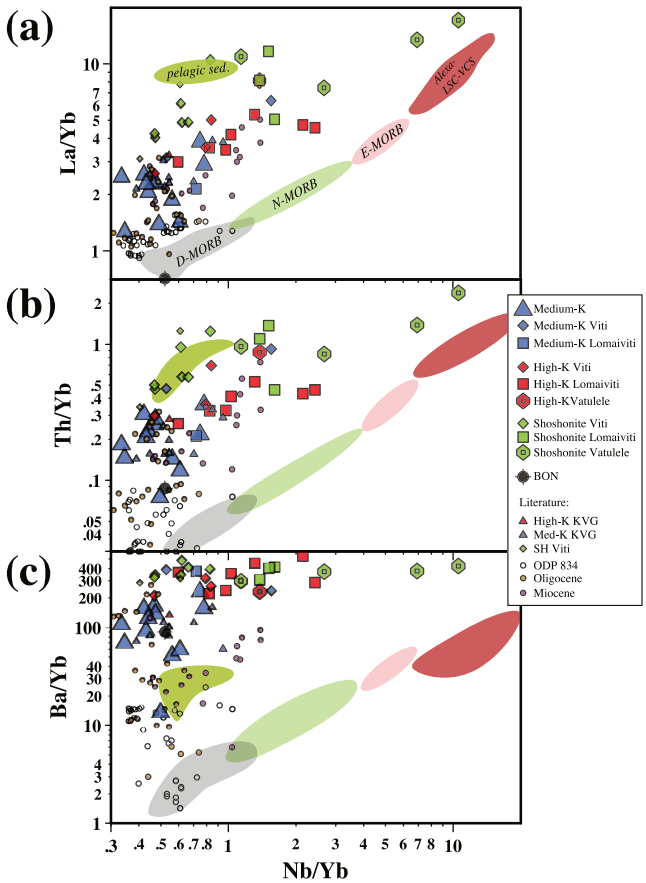

Figure 5. Nb/Yb vs. (a) La/Yb, (b) Th/Yb, and (c) Ba/Yb, reflecting increasingly fluid-mobile numerators in that order. Data and symbols as in Figure 4, omitting literature data for samples ground in WC or with Nb/Ta <10 or both. The MORB fields are for the East Pacific Rise from Niu et al. (2002) and Yang et al. (2020); NMORB is defined as having La/Sm_N = 0.8–1.5. The fields for pelagic and volcaniclastic sediments (VCS) are end-members from DSDP Site 204 (S. Turner et al., 1997). A slab-derived sediment component will lie between them. The Alexa-LSC-VCS field on the extension of the MORB trend includes data from Finlayson et al. (2018) and A. A. Price et al. (2022) for Alexa-type seamounts, and Beier et al. (2011) for the Louisville Seamount Chain from which the volcaniclastic sediments at Site 204 were derived. Data for ODP Site 834 basalts are from Hergt and Woodhead (2007). See Figure 4 in Gill et al. (2021) for the effects on these diagrams of adding a slab component and melting the resulting modified mantle.

et al. (2009) and G.-Z. Sun et al. (2017) provide mineral modes and analyses, and petrographic images, for representative Fijian shoshonitic rocks.

5.2. Major Elements

Compositions are shown in Figure 4. Most samples are basalt and a few are andesite. Our medium-K rocks from Vanua Levu have slightly lower K_2O and P_2O_5 relative to MgO than their coeval analogs in the Lau Islands, and lower than in Namosi that is more rearc. All are typical arc rocks, and they have higher K_2O but lower TiO_2 than the coeval basalts in ODP Site 834 east of the Lau Ridge. That is, the basalts erupted closer to the trench were less arc-like.

There are no consistent compositional differences between the high-K rocks of different lineaments. However, the shoshonites in Viti Levu and the Astrolabes have a few wt.% higher SiO_2 than those in Lomaiviti and Vatulele. Notably, the shoshonitic rocks have Na_2O contents relative to SiO_2 that are similar to the medium-K and high-K rocks, and even lower than in N-MORB. The positive correlation between Na_2O and Nb is similar to that in D-MORB (not shown), indicating strong source depletion despite enrichment in K_2O.

5.3. Trace Elements

All suites have characteristic arc-type enrichments of Cs, Rb, Ba, U, Pb, and Sr relative to Th + REE, and depletions of Nb, Ta, Zr, and Hf (Figures 5 and 6). Remarkably, the medium-K basalts, and even the shoshonites from Viti Levu, have as much relative Nb-depletion as in D-MORB (Nb/Yb ratios < 0.8), underscoring the strongly depleted mantle from which they came. That level of Nb-depletion has characterized Fiji throughout its history, as shown for the Oligocene and Miocene rocks in the figures. However, its extent varies between lineaments, being greatest for Viti Levu, intermediate in most of Lomaiviti, and least in the Vatulele-Beqa and Astrolabe areas plus two high-K volcanoes in Lomaiviti (Namenalala and Batiki). This geographic difference also is seen in olivine-hosted melt inclusions (Leslie et al., 2009), so is not related to crystal accumulation.

The shoshonitic rocks have the greatest relative enrichment in Rb, Ba, Sr, and Pb as well as K, but the differences in other incompatible elements between high-K and shoshonitic samples is irregular with substantial overlap. The pattern of enrichment in the medium-K basalts is similar to that of earlier Fijian volcanics. However, the level of K, Rb, Sr, Ba, LREE, and Th enrichment in the shoshonites is without precedent in Fiji, is greater than in the Quaternary Tonga or Kermadec arcs, and even exceeds that in south Pacific pelagic sediments for Ba (Figure 6; cf. S. Turner et al., 1997). The large enrichments of Pb and U relative to Ce and Nb, respectively (Ce/Pb < 7; Nb/U < 10), is most pronounced in the shoshonites, but U is enriched relative to Th in all suites, with Th/U = 1.5–2.5. The least Pb and U enrichment is in the least Nb-depleted samples from Vatulele ± Namenalala and Batiki, noted above.

REE patterns for all suites are shown in Figure 6. Those of the medium-K basalts are almost flat with a subtle maximum at Nd-Sm in some samples. Patterns of the high-K and shoshonitic samples are LREE-enriched and overlap. The Cikobia boninites have the usual U-shaped pattern with a minimum at Nd. All suites have flat HREE patterns like MORB with Dy/Yb increasing from 1.6 to 1.9 with increasing MgO, reflecting greater modal clinopyroxene. Only Vatulele shoshonites have steeper HREE patterns, with Dy/Yb of 2.2–2.3. Our data for shoshonitic samples confirm earlier results from fewer centers (Gill, 1970; Leslie et al., 2009; Rogers & Settlefield, 1994; G.-Z. Sun et al., 2017).

10.1029/2022GC010663

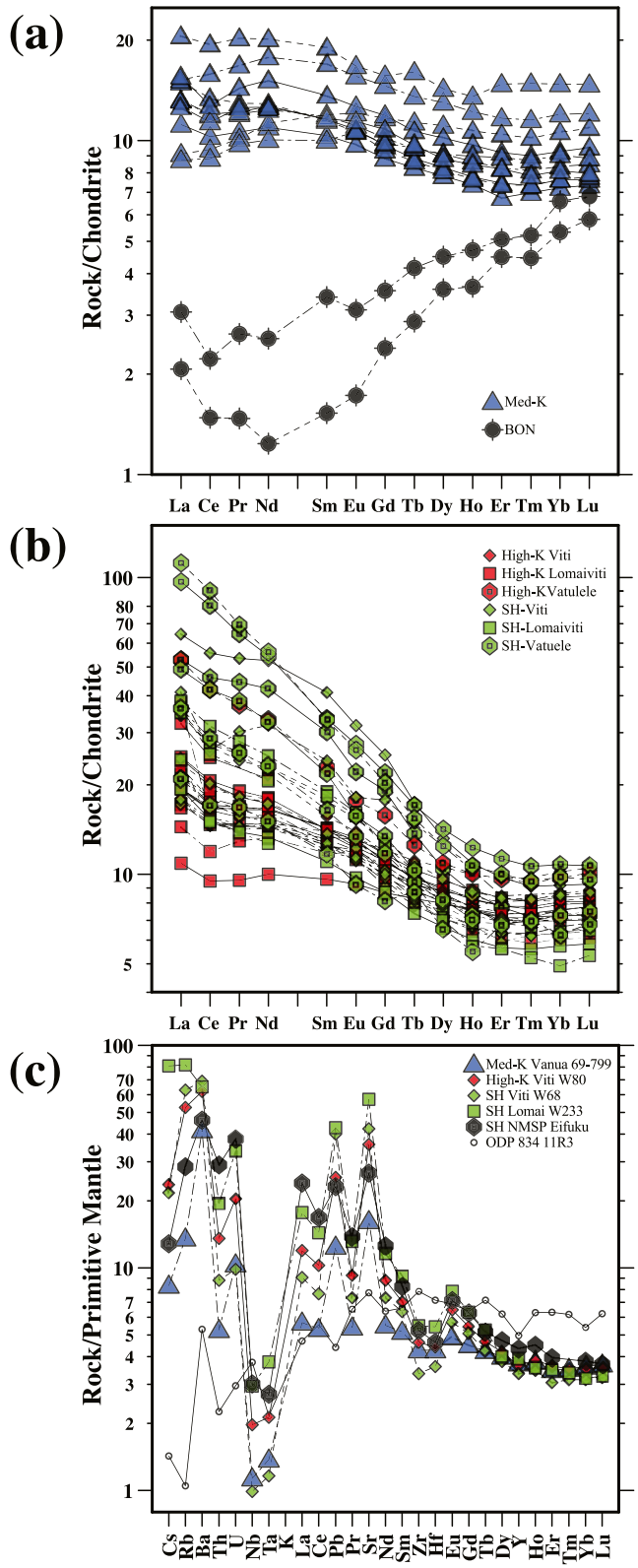

Figure 6.

The depleted nature of the Fijian shoshonites sets them apart from other intra-oceanic examples including the Northern Seamount Province in the Marianas (Fryer et al., 1997; Gribble et al., 1998; Stern et al., 1993; Tollstrup & Gill, 2005) and the Miocene South Fiji Basin (Mortimer et al., 2021). Both of those suites have higher Nb/Yb ratios and much greater LREE-enrichment than Fiji (Figure 6c). They also have Ba > Sr rather than the reverse in Fiji. The Fijian shoshonites have even more negative Zr-Hf anomalies than in the Northern Marianas, and lack the latter's high Nb/Ta ratios that were attributed to a lithospheric origin (Pearce et al., 2005).

Although the basalts in ODP Site 834 basalts are the same age as the breakup basalts, and erupted only a few tens of km trenchward of them, they have much less arc-type trace element enrichments and depletions. They have similarly low Nb/Yb ratios, strong LREE-depletion, much less positive Cs, Rb, Ba, Th, U, K, and Sr anomalies, and no negative Zr-Hf ones (Figure 6). The only similar breakup basalts are from Cikobia that also lay trenchward of the rest prior to rotation (Figure 2). The arc component somehow by-passed both.

5.4. Radiogenic Isotopes

Figure 7 shows the rough positive correlation between Nd and Hf isotope ratios that are the least likely to be affected by a slab component and, instead, the most likely to record the ambient mantle wedge. Almost all breakup basalts have similar $^{176}Hf/^{177}Hf$ ratios (~0.28315–20) that are similar to those of the Miocene volcanic and plutonic rocks that preceded them in Fiji, but higher (more depleted) than the Oligocene volcanics erupted prior to opening of the South Fiji Basin. The medium-K basalts straddle the Hf-Nd isotope Terrestrial Array of Vervoort and Blichert-Toft (1999) whereas the high-K and shoshonitic suites lie above it. In that sense, they are more "Indian" than "Pacific" in character. This contrasts with the Oligocene volcanic rocks from Fiji, and the Havre Trough, South Fiji Basin, and ODP Site 834 that all lie below the Terrestrial Array and are decidedly "Pacific" (Figure 7; Hergt & Woodhead, 2007; Gill et al., 2021; Marien et al., 2022; Todd et al., 2012). Collectively, these suites below the Terrestrial Array reflect the pre-breakup ambient mantle. The Fijian rocks with less depleted Hf and Nd isotope ratios in Figure 7a are the less Nb-depleted samples from Vatulele and Lomaiviti (see below). All the Fijian suites have higher Nd and Hf isotope ratios than do the more enriched Northern Mariana and South Fiji Basin shoshonites (not shown: Mortimer et al., 2021; Tollstrup & Gill, 2005) which is consistent with the more depleted trace element ratios of the Fijian rocks discussed above.

Figure 7a includes a field for the 7–12 Ma Colo plutonics that range from gabbro to tonalite (Marien et al., 2022). It includes data for just the pluton suites that were interpreted as being mostly differentiates of mantle derived basaltic parents, that is, those with light-depleted or flat REE patterns. They overlap the medium-K breakup basalts. In contrast, samples of LREE-enriched plutons, that were interpreted as having assimilated more crust, have higher $^{143}Nd/^{144}Nd$ at similar $^{176}Hf/^{177}Hf$, and overlap the older Fijian volcanics.

In contrast, Figure 8 shows Pb and Sr isotope ratios that are more likely to reflect the slab component. $^{206}Pb/^{204}Pb$ ratios are highest in the shoshonites from Viti Levu and adjacent Lomaiviti (Wakaya and Vatu-i-cake), whereas $^{87}Sr/^{86}Sr$ ratios are highest in the Cikobia boninite and all Lomaiviti suites, and lowest in the medium-K basalts. Although the similarly high $^{87}Sr/^{86}Sr$ in some Oligocene volcanics may reflect post-eruption seawater alteration, the Lomaiviti results are a primary feature. The $^{206}Pb/^{204}Pb$ ratios are above levels for N-MORB, in the range of E-MORB, and approach FOZO values.

Figure 9 combines elements of the previous two figures and shows that, as usual in arcs, there is mixing between depleted and enriched components, and $^{87}Sr/^{86}Sr$ is elevated above $^{143}Nd/^{144}Nd$ compared to MORB and OIB. The lower $^{143}Nd/^{144}Nd$ in the high-K, shoshonitic, and boninite suites is again apparent, and is accompanied by higher $^{87}Sr/^{86}Sr$. The overall enrichment is greater than at the Quaternary volcanic front of Tonga and most of Kermadec (not shown). The Vatulele shoshonites and Namenalala high-K rocks with high Nb are, again,

Figure 6. (a and b) REE normalized to ordinary chondrites (Nakamura, 1974). Data and symbols as in Figure 4. Literature data are not shown but are similar. Much of the vertical variation reflects differentiation. (c) Multi-element patterns of representative samples from Table 2, ODP Site 834 (12R3, 66–71: Hergt & Farley, 1994), and the Northern Mariana Seamount Province (Eifuku D31-1-6: Bloomer et al., 1989; Peate & Pearce, 1998) relative to Primitive Mantle (S.-S. Sun & McDonough, 1989). All samples have 7–10 wt.% MgO. Shoshonites from two different lineaments are shown to illustrate the diversity within Fijian categories. Note that the breakup basalts have typical arc-like enrichments of Cs, Rb, Ba, U, Pb, and Sr relative to Th + REE, that are in turn enriched relative to Nb, Ta, Zr, and Hf, whereas ODP Site 834 basalts have much less enrichment amidst greater scatter (cf. Figure 5). The Northern Mariana shoshonites are less depleted in Y + REE and less enriched in Sr, Pb, Ba, and alkalies than their Fijian counterparts.

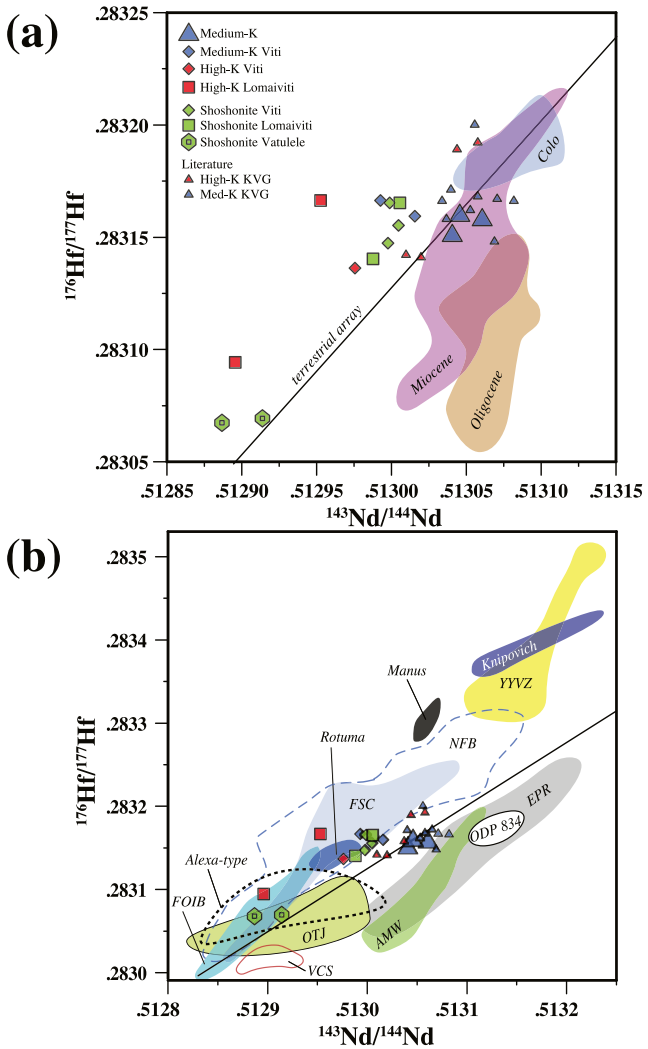

Figure 7. $^{143}Nd/^{144}Nd$ vs. $^{176}Hf/^{177}Hf$: the mostly mantle component. (a) Data and symbols as in Figure 4, plus a field for Fijian Colo plutonics from Marien et al. (2022). The Terrestrial Array is from Vervoort and Blichert-Toft (1999). (b) Data as above plus fields for the NFB, North Fiji Basin (A. A. Price et al., 2016, 2014); FSC, Futuna Spreading Center and YYVZ, Yasawa-Yadua Volcanic Zone (A. A. Price et al., 2017); VCS, volcaniclastic sediments from the Louisville Seamount Chain in DSDP Site 204 (Hergt & Woodhead, 2007; Pearce et al., 2007); EPR, East Pacific Rise MORB (Class & Lehnert, 2012; Salters et al., 2011); AMW, Ambient Mantle Wedge for the Vitiaz Arc and South Fiji Basin OIB (Todd et al., 2011); ODP Site 834 (Hergt & Woodhead, 2007); Rotuma, FOIB (Fijian OIB), and the Alexa-type seamounts of the Samoan Seamount Chain (Finlayson et al., 2018; Hart et al., 2004; A. A. Price et al., 2022, 2017); OTJ, Ontong Java Plateau (Tejeda et al., 2004, without age correction); the Manus Basin (Woodhead et al., 2001); and the Knipovich segment of the Arctic Mid-Atlantic Ridge (Sanfilippo et al., 2021). Data for volcanic rocks with SiO_2 >60% are excluded.

exceptions. Their Sr as well as Nd isotope ratios are more similar to E-MORB and OIB, that is, to basalts with old enrichments (EM2) instead of recent slab components.

Figures 10a and 10c show only spiked Pb isotope ratios. In none of the Fijian samples is $^{207}Pb/^{204}Pb$ as high relative to $^{206}Pb/^{204}Pb$ as at the Kermadec volcanic front (not shown: Gill et al., 2021; Timm et al., 2014), reflecting little if any direct or indirect recycling of continentally derived material in Fiji. The least radiogenic Pb is in the medium-K basalts and lies within the field of previous Fijian Pb near the Northern Hemisphere Reference Line (NHRL) of Hart (1984). The same is true of a high-K basalt and shoshonite from the Vatulele lineament that are the least Pb-enriched (lowest Ce/Pb) of these rock types. Breakup basalts have higher $^{206}Pb/^{204}Pb$ than in most Pacific N-MORB but similarly low $\Delta^{207}Pb$ and $\Delta^{208}Pb$ as defined by Hart (1984), which is why the Fijian mantle has long been considered to be from inherently "enriched" mantle (Gill, 1984; Todd et al., 2012). Pb in most Fijian igneous rocks of all ages, and especially in the Viti Levu shoshonites, have higher $^{206}Pb/^{204}Pb$ than do mixtures of the usual mixing components of subducting crust of the Pacific Plate; that is, pelagic sediment and altered MORB (Figures 10b and 10d: S. Turner et al., 1997). An additional high-$^{206}Pb/^{204}Pb$ source component is required. This requirement is even more extreme than for the atypical volcanoes at the Kermadec front for which a contribution of Pb from subduction of seamounts on the Hikurangi Plateau has been invoked (Timm et al., 2014). The Pb in the high-K basalts of Lomaiviti and Lau is noticeably more enriched in $^{208}Pb/^{204}Pb \pm {}^{207}Pb/^{204}Pb$ with respect to $^{206}Pb/^{204}Pb$ (i.e., they have higher $\Delta^{207}Pb$ and $\Delta^{208}Pb$) than anything earlier in Fiji (Figures 10a and 10c).

6. Discussion

6.1. Temporal and Spatial Patterns

Our new geochemical data confirm that Fijian volcanism during arc breakup continued to be characterized by subduction-related compositions up to 3 Ma, as previously documented (e.g., Gill et al., 1984; Gill & Whelan, 1989a; Leslie et al., 2009; Rogers & Settlefield, 1994; G.-Z. Sun et al., 2017). Indeed, the 7–3 Ma medium-K basalts are typical of volcanic fronts ~125 km above a slab. This suggests but does not prove that subduction itself continued beneath Fiji during this time even while it began to rotate counter-clockwise and the Lau Basin started to open (Figure 2; Malahoff, Hammond, et al., 1982; G. K. Taylor et al., 2000).

As a result, we recognize four stages in the geochemical evolution of the Vitiaz Arc. The first lasts from subduction initiation until opening of the South Fiji Basin (Todd et al., 2012). It is shown by the "Oligocene" samples in our figures and includes "Eua" in Tonga and the Yavuna Group in Fiji. Its ambient mantle wedge was "Pacific" isotopically, it was relatively undepleted with lower Nd and Hf isotope ratios (Figure 7), and it had a relatively small mass fraction of LREE- and Th-bearing slab component (Figure 5). In that respect it was like the modern Tongan volcanic front. The second stage post-dates opening of the South Fiji Basin and is shown by the "Miocene" samples in our figures that come from the Lau Volcanic and Wainimala Groups. Although they remain "Pacific" isotopically, their ambient mantle was more depleted with higher Hf isotope ratios (Figure 7). They are characterized by more relative enrichment in LREE and Th than in the first stage (Figure 5), and they are closer to the Hf-Nd Terrestrial Array in Figure 7, indicating the addition of a more melt-like slab component, as previously recognized by Hergt

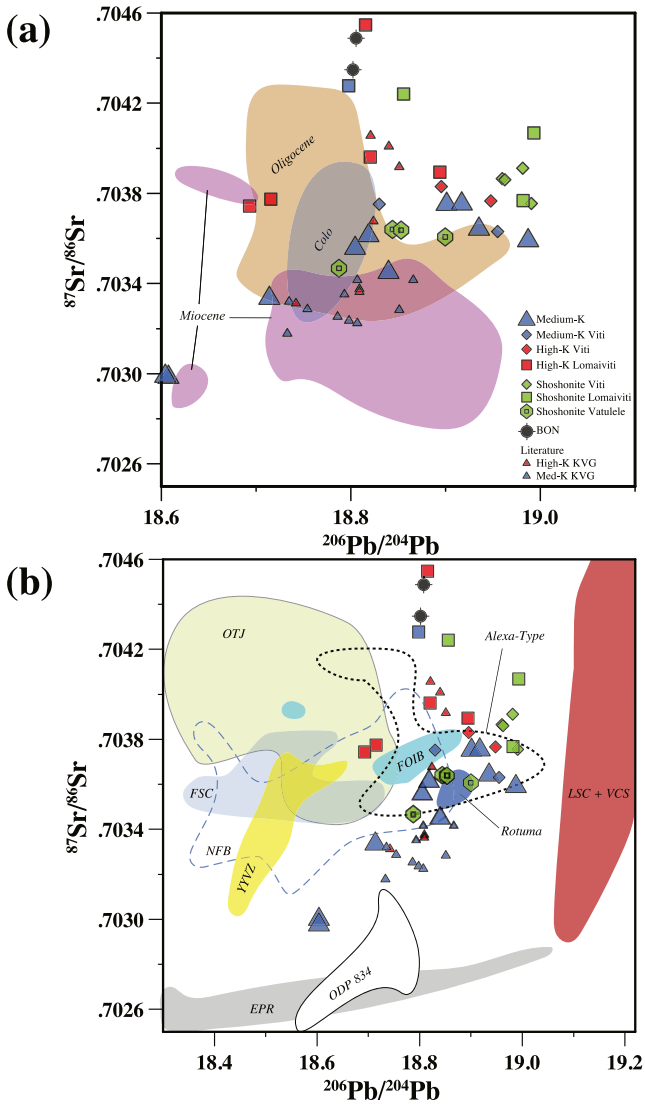

Figure 8. $^{206}Pb/^{204}Pb$ vs. $^{87}Sr/^{86}Sr$: the mostly slab component. Data, symbols, fields, and data sources as in Figure 7 where smaller symbols are from the literature. Unspiked Pb data are included, and unleached samples are shown whenever possible, but all Alexa-type and Ontong Java samples were leached to some extent before digestion. The two small purple fields in (a) are for atypical Fijian Miocene rocks. Some Samoan basalts with high $^{3}He/^{4}He$ plot at the top right corner of (b) (e.g., from Ofu: Jackson et al., 2007), but most have higher $^{87}Sr/^{86}Sr$ than in this figure as do pelagic sediments.

and Woodhead (2007). The third stage accompanies arc breakup and is characterized by a slab component derived from subducted Alexa-type Samoan seamounts ± Pb from Louisville seamount material in Viti Levu shoshonites. The final stage abruptly post-dates arc breakup and is characterized by basalts from a new "Indian" mantle in the backarc basins, Fijian OIB, and along the Vitiaz Trench Lineament (e.g., Rotuma). This final stage is visibly offset from the first three in Figure 12 that combines Hf-Nd isotope and concentration anomalies. It shows that the ambient mantle of the first three stages remained broadly similar apart from becoming more depleted after opening of the South Fiji Basin.

Spatially, our new data confirm that the magnitude of subduction-related geochemical features decreased west to east during the third stage, from shoshonitic closest to where the arc broke, through high-K to low-K and boninitic in the east. Shoshonitic and high-K centers are spatially separate on the Viti Levu lineament, with the latter lying 20–30 km north of the former. They are interspersed along the Lomaiviti and Vatulele-Beqa lineaments. K-Ar ages are oldest (4.0–5.2 Ma) for the shoshonitic centers on the western portions of the Viti Levu (Nausori and Tavua) and Vatulele lineaments, and younger (3–4 Ma) further east (Malahoff, Hammond, et al., 1982; Whelan et al., 1985). There is a similar apparent eastward younging amongst the medium-K basalts of Vanua Levu, although the age differences are small. The oldest volcanic rocks (~7 Ma) are the boninitic ones from Cikobia, and the nearby low-K Udu rhyolites in northeastern Vanua Lavu (Whelan et al., 1985).

We noted earlier that the Nb/Yb ratios of the shoshonites on Viti Levu are lower than in outlying islands. Viti Levu is not only the largest Fijian island, but also the most uplifted during breakup and it exposes many tonalitic plutons (Marien et al., 2022). We attribute the Nb-depletion, uplift, and plutonism to focused mantle melting and basalt intrusion into the crust near the site of arc breakup. If so, then any subsequent slab component should have its maximum expression there because the mantle would be most depleted.

The medium-K basalts and andesites merit special comment. Our new data for rocks from the Natewa Formation on Vanua Levu are similar in age and composition to those from the Korobasaga Volcanic Group on the Lau Islands (Cole et al., 1985, 1990; Gill, 1976; Hergt & Woodhead, 2007). These two groups define the Pliocene volcanic front of the Vitiaz Arc that remained active while the Tonga Trench started to roll-back to form what became the intervening Lau Basin. Although that basin is now a backarc basin between the Quaternary Tonga Arc volcanic front and the Lau Ridge remnant arc, from 5 to 3 Ma it was a forearc basin trenchward of the Natewa-Korobasga volcanic front. The Korobasaga rocks are distinguished from their predecessors, the Lau Volcanic Group, by their lower Zr and higher Sr contents (Gill, 1976), a trait that is shared by our new data for Vanua Levu. This combination suggests a higher degree of flux melting for the Korobasaga rocks in which more flux adds the Sr and more melting lowers the Zr. The Vanua Levu medium-K rocks extend to even more radiogenic Sr and Pb isotope ratios than in most Korobasaga rocks, and to less radiogenic Nd, indicating more slab-derived component closer to the breakup site. Neither is as depleted in LREE and HFSE relative to HREE, nor as isotopically "Indian", as in the modern central Tonga arc (Hergt & Woodhead, 2007). However, both are much more arc-like than the basalts at ODP Site 834. The latter have "Pacific"-type isotopes (Figures 7–10) and similarly low Nb/Yb and high $^{176}Hf/^{177}Hf$ ratios as the arc (i.e., their mantle source was comparably depleted), but they have less enrichment in Ba, Th, and La (Figures 5 and 6). Therefore, the same old ambient mantle remained beneath the Vitiaz Arc until ~3 Ma, but much less slab fluid was added to it in the forearc.

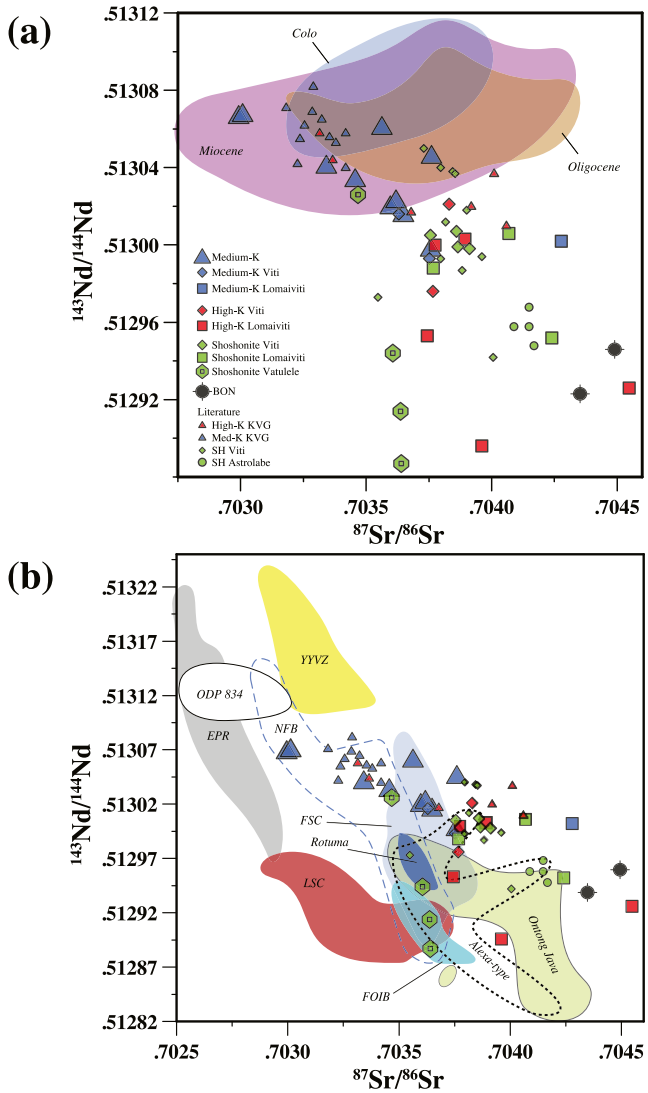

Figure 9. $^{87}Sr/^{86}Sr$ vs. $^{143}Nd/^{144}Nd$. Data, symbols, fields, and data sources as in Figures 7 and 8. Note in (b) that the "new mantle" is offset to higher $^{87}Sr/^{86}Sr$ relative to $^{143}Nd/^{144}Nd$ than the EPR, most LSC, and ODP Site 834. The Viti Levu shoshonitic sample with an atypically low $^{143}Nd/^{144}Nd$ like that of the Astrolabes is from a Tavua-related monzonite sill (Rogers & Settlefield, 1994). The high-K KVG basalts with atypically high $^{87}Sr/^{86}Sr$ also have high the highest $^{208}Pb/^{204}Pb$ ratios. Most Samoan basalts lie off this figure to the lower right.

With few exceptions, the shoshonitic suite has the maximum enrichment in K, Rb, Cs, Sr, U, and Pb relative to MgO and REE (Figures 4–6) which usually is attributed to more slab-derived fluid. However, they also have higher Th (Figure 5b), and lower $^{143}Nd/^{144}Nd$ with respect $^{176}Hf/^{177}Hf$ ratios (Figure 7) that broadly correlate negatively with light REE-enrichment (Figure 11) and Zr, Hf-depletion relative to middle and heavy REE in our samples (Figure 6). This suggests more transport of LREE than Zr, Hf in the slab component behind the volcanic front and near the tear, presumably in a melt or super-critical fluid. Hergt and Woodhead (2007) made a similar point when comparing the KVG to modern Tonga. That is, the source of all breakup basalts was affected by addition of a higher temperature slab component than in modern Tonga. Because the shoshonites are isotopically similar to, as well as spatially interspersed with, the high-K basalts, the differences between them are mostly related to the cumulative degree of melting of similar sources (Gill & Whelan, 1989a; Leslie et al., 2009). If the medium-K basalts represent the highest percent melting, then the degree of melting was lower close to where the arc broke and higher at the volcanic front.

None of these suites erupted in central Viti Levu where tonalitic plutons had intruded several million years earlier (7–12 Ma: Gill & Stork, 1979; Marien et al., 2022). We speculate that the crust there was too thick and ductile for basalt magmas to penetrate. The medium-K Namosi Andesite on the southeastern edge of the plutons is an exception. Although our sample of it is more enriched in Nb, LREE, and Th than the other medium-K samples in this paper (Figure 5), its isotope ratios are similar.

The boninitic high-Mg andesites and medium-K basalts of Cikobia are the oldest rocks of this study, the furthest from the breakup with Vanuatu, the closest to the forearc rifting that led to the Lau Basin, and near the arc's pole of rotation. We interpret them as an early volcanic expression of the impending breakup. The boninite's Th/REE ratios are as low as in modern Tonga and they have positive Zr-Hf anomalies (Hf/Sm ~2) above their U-shaped REE patterns (Figure 6). Although they have low Ti, Na, Y, and HREE contents, they are not enriched in Sr; that is, they are not adakitic. Instead, they indicate shallow, high-degree melting of depleted peridotite fluxed by a slab melt, as inferred for their Tongan analogs (Falloon et al., 2008). Their unusually low $^{143}Nd/^{144}Nd$ and high $^{87}Sr/^{86}Sr$ ratios reflect this relatively large slab melt contribution. In contrast, the basalts have the lowest K, Rb, Ba, Pb, Th, and U, and the least radiogenic Sr and Pb in this study. The pre-rotation location of Cikobia lay tens of km trenchward of the location of other medium-K basalts (Figure 2), as did the ODP Site 834 basalts to which they are most similar. Consequently, the pillow lavas of this small island have the least, and most, slab component of the breakup basalts. Unfortunately, the stratigraphic relationships are unknown because the samples were collected by different people at different times.

6.2. Sources During Breakup

The greatest change in magma sources affecting the Fiji area during the Neogene was the isotopic shift from old "Pacific" to new "Indian" mantle following breakup of the Vitiaz Arc. The ambient mantle beneath the Vitiaz Arc was "Pacific" from its inception to upper Miocene (Gill et al., 2021; Todd et al., 2012). The change results in higher $^{87}Sr/^{86}Sr$ and $^{176}Hf/^{177}Hf$ with respect to $^{143}Nd/^{144}Nd$, higher $^{208}Pb/^{204}Pb$ with respect to $^{206}Pb/^{204}Pb$, and lower $^{206}Pb/^{204}Pb$ in the basalts. The change was first discovered, and the names were first applied, during ODP drilling in the Lau Basin where the oldest basalts (4–5 Ma at Site 834) remain isotopically "Pacific", but everything <3 Ma is "Indian" (Hergt & Hawkesworth, 1994; Hergt & Woodhead, 2007). Young basalts

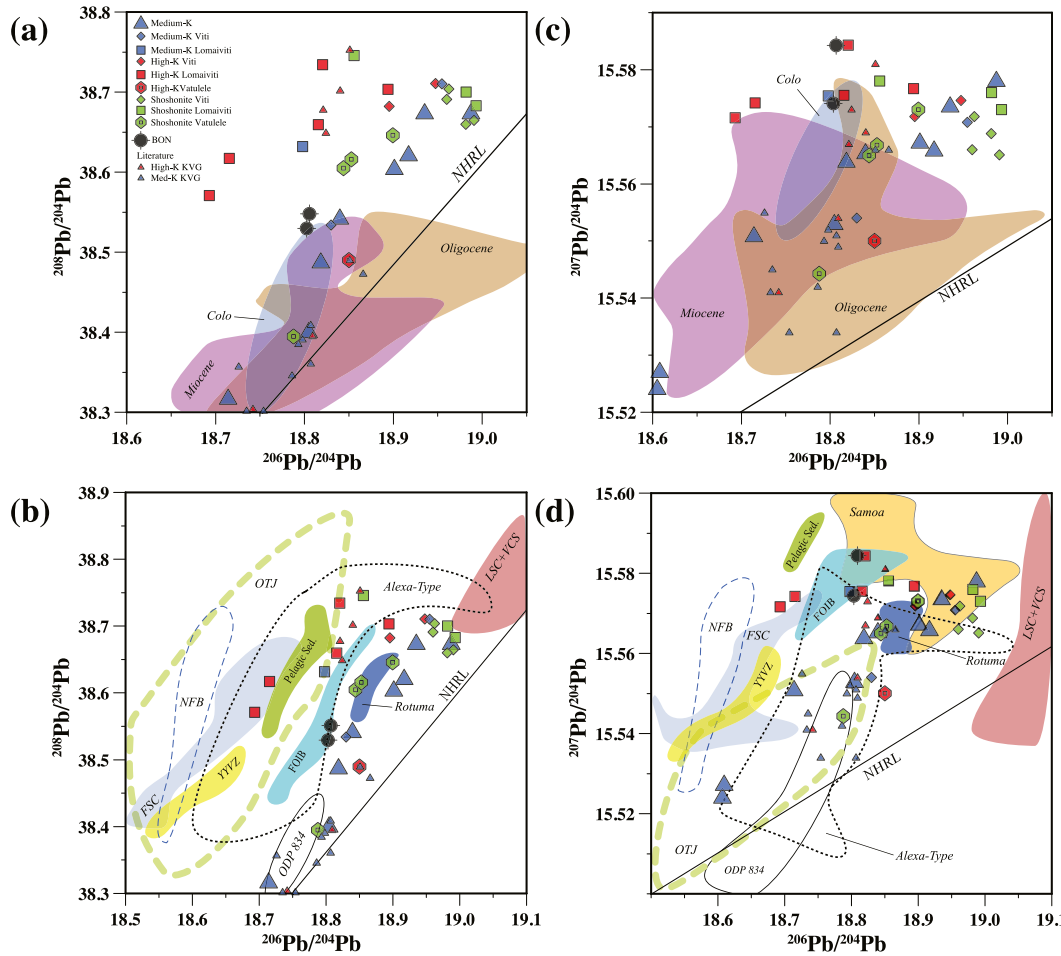

Figure 10. $^{206}Pb/^{204}Pb$ vs. (a, b) $^{208}Pb/^{204}Pb$, and (c, d) $^{207}Pb/^{204}Pb$. Data, symbols, field, and data sources as in Figure 7. Only spiked data are shown except for Alexa-type, OTJ, and the pelagic and volcaniclastic sediments from DSDP Site 204. NHRL is the Northern Hemisphere Reference Line from Hart (1984). (a) The high-K and shoshonitic samples near the NHRL are from the Vatulele lineament. The two high-K basalts furthest above the NHRL at low $^{206}Pb/^{204}Pb$ are from Moala and Matuku in southernmost Lomaiviti. (c and d) as above.

dredged from all parts of the Lau and North Fiji Basins are "Indian" (e.g., Pearce et al., 2007; A. A. Price et al., 2016, 2014, 2017), as is the mantle wedge now beneath Tonga (Hergt & Woodhead, 2007). Is this new mantle the cause or the effect of arc breakup?

At first glance, the Nd-Hf isotopes of the high-K and shoshonitic rocks, and the medium-K Namosi andesites, differ from what came before them, and appear "Indian" by lying above the Terrestrial Array in Figure 7. This implies that the new mantle had already displaced the previous "Pacific" ambient mantle wedge by ~6 Ma when the Namosi rocks appeared. Because the Colo plutons that have the least crustal component (e.g., Korolevu) are isotopically similar to the medium-K Pliocene basalts, although not as extreme as Namosi and the shoshonites (Figure 7), the new mantle might have been present as early as 10 Ma. However, the apparently "Indian" character of the breakup basalts is deceiving because Figure 5 shows that their LREE like La (and Nd) are enriched relative to Nb/Yb, consistent with having been added by a slab-derived component. If the added Nd is unradiogenic, then the only change from before is the presence of more sediment-derived LREE in the slab component added to the depleted ambient mantle. Its Hf isotope ratios remain high and its Nb/Yb ratios remain low.

This also is seen in Figure 11 which illustrates the complexity of the topic. $^{143}Nd/^{144}Nd$ and La/Yb correlate negatively as expected for mixing between depleted mantle and a sediment-rich slab component, or enriched mantle (EM2). Many breakup basalts overlap data for, and extend to more enriched compositions than, earlier Fijian volcanics. Although most of the shoshonitic samples are offset to *higher* La/Yb than the medium-K and

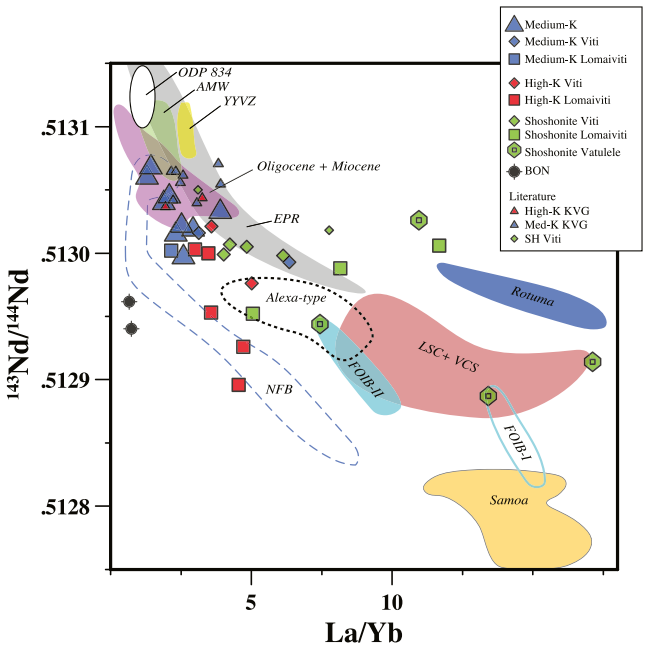

Figure 11. La/Yb vs. $^{143}Nd/^{144}Nd$, showing that some of the variation in $^{143}Nd/^{144}Nd$ in breakup basalts is related to source fertility. Literature data as in previous figures but only for basalts with >4.5 wt% MgO. EPR data overlap the Fijan Ambient Mantle Wedge (AMW) and ODP 834 fields, whereas the lower $^{143}Nd/^{144}Nd$ relative to La/Yb in the North Fiji Basin is an intrinsic difference, and is shared by the three high-K Lomaiviti basalts that also are Nb-enriched. The two types of Fijian OIB (FOIB-I, II) are basanitic and hawaiitic, respectively (Gill & Whelan, 1989b). The higher La/Yb in some shoshonites and Rotuma reflect lower percent melting.

high-K breakup basalts, and older Fijian volcanics, that can be explained by smaller degrees of melting for the shoshonites. Conversely, all Fijian samples other than shoshonites have *lower* La/Yb relative to $^{143}Nd/^{144}Nd$ than EPR MORB, and that can be explained by greater prior depletion of the ambient arc mantle wedge. If so, then little changed during breakup except for more slab-derived LREE added to the mantle wedge and lower percent melting near the tear.

This conclusion is more forcefully shown in Figure 12 that combines Hf and Nd isotope and concentration data in a way that was introduced by Pearce et al. (1999) and applied to the southwest Pacific, including rock suites discussed in this paper, by Hergt and Woodhead (2007) and Pearce et al. (2007). See its figure caption for details. The main conclusion is that the position of the breakup basalt data relative to the Terrestrial Array (i.e., their apparent "Indian-ness") correlates positively with their relative LREE-enrichment—for example, how far their La/Yb ratio is above the MORB-OIB line in Figure 5a, or their LREE are above Zr and Hf in Figure 6c. The breakup basalts, like all earlier Fijian volcanics, lie within the field identified as the Pacific Domain by Pearce et al. (2007) and were derived from old Pacific-type mantle to which an LREE-rich slab component was added.

In Figure 12, the Oligocene volcanics that predate opening of the South Fiji Basin, and the 4–5 Ma basalts in ODP Site 834, both reflect the old "Pacific" mantle. Neither has much slab component, as also can be seen in Figures 5 and 6. The Miocene volcanics and medium-K breakup basalts straddle the Hf-Nd isotope Terrestrial Array, as also can be seen in Figure 7a. This figure makes clear that the magnitude of the Nd isotope displacement of the breakup basalts above the Terrestrial Array (i.e., their apparent "Indian-ness") correlates positively with their relative LREE-enrichment; for example, how far their La/Yb ratio is above the MORB line in Figure 5, or their LREE are above Zr + Hf in Figure 6c. Because the breakup basalt data project back to the 0, 0 intersection in Figure 12, they are derived from old "Pacific" mantle to which an LREE-rich slab component was added. The breakup basalts, like all earlier Fijian volcanics, lie within the trend identified as the Pacific Domain by Pearce et al. (2007) and as Lau Island-Kermadec by Hergt and Woodhead (2007). The big change in the ambient mantle comes after arc breakup. The North Fiji Basin basalts are clearly from new "Indian" mantle even though the basalts have positive Hf concentration anomalies. They lie between the fields of the North and Central Tonga arcs, and the North and Central Lau Spreading Centers by those authors. All are <3 Ma, and they reflect the arrival of new ambient mantle. The most extreme relative Hf isotopic enrichment is in the very depleted basalts from the YYVZ.

However, note in Figure 7a that one Lomaiviti high-K basalt (from Namenalala) and two shoshonites (from Vatulele) have lower $^{143}Nd/^{144}Nd$ and $^{176}Hf/^{177}Hf$ than the rest. They also are characterized by higher Nb/Yb, Nb/U, and Ce/Pb ratios, ruling out additional subduction components as the cause. Instead, they are more like OIB basalts. Figure 11 shows that they resemble basalts of the North Fiji Basin, Rotuma, and the <3 Ma Fijian OIB-like basalts (FOIB) (Gill & Whelan, 1989b; A. A. Price et al., 2017). Indeed, Namenalala Island lies midway between two of the largest FOIB volcanoes, Seatura in southwest Vanua Levu, and Koro Island in Lomaiviti. Therefore, some new mantle seems to have been present as early as 4.7 Ma, the age of Vatulele, on the outskirts of Viti Levu. The higher La/Yb in shoshonites and some other samples in Figure 11, like FOIB-I that are basanites, just reflects lower percent melting.

Figure 11 also shows that these somewhat OIB-like high-K and shoshonitic basalts with the lowest $^{143}Nd/^{144}Nd$ ratios share traits with seamounts on the Pacific Plate that would have been near the tear just prior to or during the breakup. Specifically, they are most similar isotopically to basalts from the Alexa-type seamounts of the Samoan chain, and the LSC and volcaniclastic sediments derived therefrom. That is, seamount material with

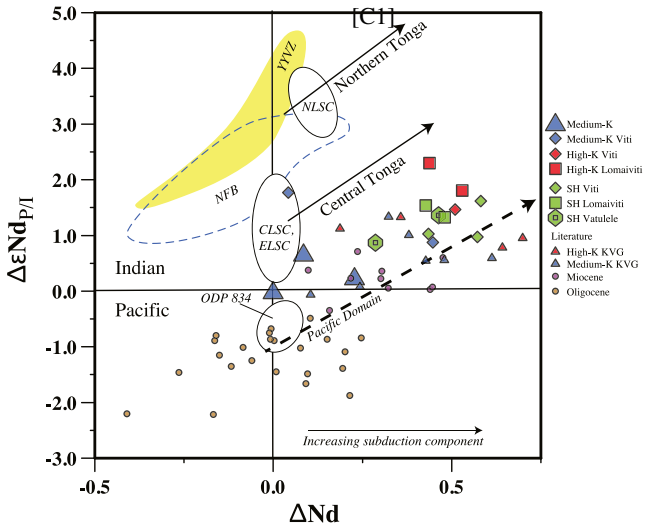

Figure 12. The *x* and *y* axes combine Hf and Nd concentration and isotope ratios, respectively, in a way that was introduced by Pearce et al. (1999). See that paper for a quantitative explanation of them. It has been applied to the southwest Pacific, including rock suites discussed in this paper, by Hergt and Woodhead (2007) and Pearce et al. (2007). Qualitatively, the *x*-axis shows the magnitude of Nd concentration anomalies relative to Hf. Positive numbers reflect positive Nd (or negative Hf) anomalies that are common in arcs, and negative numbers reflect positive Hf anomalies that are common in MORB. The magnitude of the concentration anomaly is affected both by igneous differentiation, and the amount and kind of slab component. Positive numbers were attributed to increasing subduction input in Figure 5 of Pearce et al. (2007). The vertical axis tells how far above (positive values) or below (negative ones) the isotope ratios of the same sample lie relative to a reference line in an Hf vs. Nd isotope diagram like Figure 7. Pearce et al.'s (1999) values and those in Figure 12 are relative to their line separating Indian(I) vs. Pacific(P)-type MORB that is similar to Vervoort and Blichert-Toft's (1999) Terrestrial Array that we show in Figure 7. Negative numbers identify samples below the Terrestrial Array that are "Pacific" in character, while positive numbers identify samples above the array that are "Indian" in character. The arrows labeled Pacific Domain and Central and Northern Tonga, and the data fields for NLSC, CLSC, and ELSC (North, Central and East Lau Spreading Center), are from Pearce et al. (2007). The Miocene and KVG (Korobasaga Volcanic Group) data in our figure include some from Pearce et al. (2007) and Hergt and Woodhead (2007). Breakup basalt and literature KVG data are the same as in Figure 7a. North Fiji Basin basalt data are from A. A. Price et al. (2014, 2017). This figure requires not only Hf as well as Nd isotope ratios, but also careful digestion methods to ensure that Hf and all REE are in solution. For that reason, samples with Zr/Hf > 50 are excluded.

similar $^{143}Nd/^{144}Nd$ and La/Yb ratios might have been subducted at the Vitiaz Trench close to the time that these more OIB-like breakup basalts erupted just south of the trench in Fiji.

With that in mind, we now return to Figures 7–10 and compare the isotopic characteristics of breakup basalts to those of the incoming Samoa, Louisville, and Rurutu seamount chains and the Ontong Java Plateau on the Pacific Plate, the basalts of the North Fiji Basin, the <3 Ma OIB from Fiji, and the young basalts from Rotuma on the Vitiaz Trench Lineament. We exclude basalts from the Macdonald seamount chain on the Pacific Plate that never subducted into the Tonga Trench because it lay too far to the northeast (A. A. Price et al., 2017). The multiple spreading centers in the northeast Lau Basin also lie too far east of the breakup basalts to matter.

Figure 7 shows isotopic traits that are most characteristic of the ambient mantle and least affected by the slab component. Previously we noted that the breakup basalts have similar Hf isotope ratios as the Oligocene to Miocene volcanic and plutonic rocks that preceded them, but lower Nd isotopes, especially in the shoshonitic and high-K suites. We attributed that to the addition of more slab-derived Nd to the Pacific-type ambient mantle that characterized the Vitiaz Arc from its inception. In contrast, Figure 7b shows that the Hf-Nd isotopes of <3 Ma Fijian OIB (FOIB) and those from Rotuma overlap those of the enriched basalts of the North Fiji Basin that come from, or lie north of, the Fiji Triple Junction (FTJ in Figure 1). These basalts plot along the MORB-OIB trend in Figure 5 (but are not shown) and do not have arc-type relative enrichments of La, Th, and Ba. That is, *they* are from the new "Indian"-type mantle that followed breakup of the Vitiaz Arc and, therefore, lacked a subduction component. In addition, the atypical high-Nb Fijian breakup basalts lie near the Fijian OIBs in Figures 7–11 and, therefore, also are from a source that contains some new mantle. Although some data for the Alexa-type seamounts and Ontong Java overlap those for the most enriched North Fiji Basin and Fijian OIBs, they extend to below the Terrestrial Array, as do the volcaniclastic sediments in DSDP Site 204 derived from the LSC. Although that means there is little or no Hf and Nd from these sources in most breakup basalts, there is ambiguity in this figure about whether those elements in the high-K and shoshonitic breakup basalts are from new mantle (they are most similar to the Futuna Spreading Center: A. A. Price et al., 2016) or old mantle plus slab-derived Nd. We prefer the latter interpretation because of (a) the enrichment in LREE relative to Nb/Yb in the breakup basalts (Figure 5), (b) the difference between North Fiji Basin and most breakup basalts in the relationship between LREE-enrichment and Nd isotopes (Figure 11), (c) the similarity in Hf isotopes between most breakup basalts and ODP Site 834 (Figure 7), and (d) the positive correlation between Nd concentration anomalies and the displacement of Nd isotope ratios above the Terrestrial Array (Figure 12). That is, most or all of the Hf in breakup basalts is from the old ambient mantle wedge, whereas more of the Nd is slab-derived. Our conclusion extends the arguments that Hergt and Woodhead (2007) applied to the KVG to most of the breakup basalts. The new ambient mantle extends from something at least as depleted as in the YYVZ to something at least as enriched as Ontong Java or Samoa.

Figure 8a showed that the slab-derived Sr and Pb in many breakup basalts, especially the medium-K ones, remained similar to what had characterized Fiji throughout its previous history, and that the Pb is most radiogenic in the shoshonitic and high-K rocks of Viti Levu and adjacent Lomaiviti. Those basalts are the most depleted in HFSE and HREE and, therefore, where the slab component is least diluted by ambient mantle. Figure 8b shows that this slab component could come many sources, to which could be added Samoa that has higher $^{87}Sr/^{86}Sr$ than shown in the figure. Rurutu can be excluded because its $^{87}Sr/^{86}Sr$ ratios are <0.704

when its $^{206}Pb/^{204}Pb$ ratios are >19.8. However, this is an especially difficult figure to interpret because the isotope ratios of both elements are so susceptible to both seafloor alteration and acid leaching during sample preparation. As much as possible, we show data for minimally leached samples from Ontong Java and the Alexa-type seamounts, but all were acid-cleaned to some extent before digestion. All ratios are current, not initial. The data for Fijian breakup basalts most closely match those of the Alexa-type seamounts, whereas the Pb in both the Rurutu and Louisville chains, and Sr in most of the Samoan chain, is more radiogenic. A minority of samples from Ontong Java come close, but the Pb in most of Ontong Java is insufficiently radiogenic, especially for the shoshonites that have the highest Pb contents of breakup basalts. The mis-match is greatest for the stratigraphically highest Singgalo Ontong Java basalts that would be the most likely to melt during subduction.

Figure 9b shows that Sr in most breakup basalts is mostly slab-derived, especially relative to "Pacific"-type ambient mantle. Ontong Java or any of the seamount chains could explain the slab component in this figure. However, the Sr and Nd in the most Nb-rich shoshonitic and high-K basalts need little slab component and could come largely from the new "Indian"-type mantle whose Sr is somewhat more radiogenic relative to Nd than in the previous ambient mantle.

Although at first glance the Pb isotope ratios in breakup basalts could be explained in many ways, closer inspection of Figure 10 indicates otherwise. Those with the highest $^{206}Pb/^{204}Pb$ ratios also have the highest Pb contents (i.e., the shoshonites of Viti Levu and adjacent Lomaiviti). They require a source component that lies close to the NHRL such as the basalts and volcaniclastic sediments from the LSC (Beier et al., 2011; S. Turner et al., 1997). Those with the lowest $^{206}Pb/^{204}Pb$ ratios, in the high-K basalts of southern Lomaiviti and Lau, are most similar to the Alexa-type seamounts (Hart et al., 2004; A. A. Price et al., 2022). Although they share the high $\Delta^{207}Pb$ and $\Delta^{208}Pb$ of Ontong Java and the new mantle of the North Fiji Basin, they have higher $^{206}Pb/^{204}Pb$ ratios than either. We infer that the Alexa-type Pb and Sr in breakup basalts are slab-derived because the basalts have low Ce/Pb (<5) in contrast to the later Fijian OIB that also have high $\Delta^{207}Pb$ and $\Delta^{208}Pb$ but Ce/Pb > 20 as in other intra-plate basalts. Consequently, Figure 10 may indicate that the change in Pb from pre-breakup igneous rocks in Fiji, which lies close to the NHRL, to the Pb in break-up basalts with higher $\Delta^{207}Pb$ and $\Delta^{208}Pb$, reflects a change from subducted Louisville to Samoan chain sources. Their high $\Delta^{207}Pb$ might also indicate relatively more pelagic sediment in the slab source (Figure 10d). Because post-breakup basalts have high OIB-like Ce/Pb ratios, their Pb is intrinsic to the new mantle and ranges from ratios as depleted as in YYVZ to ratios as enriched as in Ontong Java or Samoa.

Previously, Fijian Pb near the NHRL has been attributed to FOZO-type enrichments in the old ambient mantle wedge because such Pb is found in Miocene backarc basalts in the South Fiji Basin (Gill, 1984; Todd et al., 2011). That remains a viable explanation for why such Pb has characterized Fiji throughout its history, including in the Oligocene when it was far from the LSC and Hot Spot Highway, and why $^{206}Pb/^{204}Pb$ remained 18.7–19.0 in almost all Fijian volcanic rocks including those with Ce/Pb $\geq$ 25. However, because Louisville-derived volcaniclastic sediments became increasingly available for subduction beneath Fiji from the Late Miocene onward (Figure 2), and most Fijian suites have low Ce/Pb ratios, it is simpler to attribute the Pb in at least the breakup basalts to an exogenous source.

It is also instructive to comment on what the Fijian shoshonite sources are not. We noted earlier that the Fijian shoshonites differ from their neighbors in the South Fiji Basin (Figure 1; Mortimer et al., 2021) and those in the Northern Mariana Seamount Province (NMSP; e.g., Gribble et al., 1998). The former have isotope ratios similar to those of volcanic rocks in the Taupo Volcanic Zone in New Zealand and seem somehow continentally influenced. The absence of old continental crust in Fiji (Marien et al., 2022) and its distance from New Zealand account for the differences in the shoshonites. However, differences from the NMSP are more difficult to explain because those shoshonites also are attributable to recycled parts of the Hot Spot Highway, including the Samoan chain (Finlayson et al., 2018). The chief differences between Fiji and the NMSP are that Nd and Hf isotopes in the NMSP are much lower and more similar to the subducting seamounts, and their Zr + LREE concentrations are much higher (Figure 6). In contrast, the isotope ratios of more fluid-mobile Sr and Pb are quite similar in Fiji and the NMSP, apart from Pb north of 24°N in the NMSP (i.e., Iwo Jima and Fukutoku-oka-no-ba) that is more like the Rurutu Chain. This pattern can be explained by more melting of the slab beneath the NMSP, perhaps related to less oblique convergence there, or to tearing of the arc and foundering of the slab in Fiji.

Finally, although a complete review of the characteristics of the new "Indian-type" mantle that feeds the many spreading centers of the North Fiji and Lau Basins after 3 Ma is beyond our scope, one aspect merits comment. As with most mantle sources, at least two components are involved, one depleted, the other enriched. The enriched component has received the most attention and historically just been called "Samoan." It varies between spreading centers and decreases with distance from the Vitiaz Trench Lineament (Pearce et al., 2007; A. A. Price et al., 2017). However, the depleted component most defines the "Indian"-ness of the new mantle; namely, its low $^{206}Pb/^{204}Pb$, high $\Delta^{208}Pb$, and high $^{176}Hf/^{177}Hf$ with respect to $^{143}Nd/^{144}Nd$. It has some of the highest $^{176}Hf/^{177}Hf$ ratios on Earth at the YYVZ segment only 100 km north of Fiji (Figure 1; A. A. Price et al., 2014). They are as high as those in basalts of the Knipovich segment of the Arctic Mid-Atlantic Ridge that are interpreted as reflecting ultra-depleted asthenosphere (Figure 7b; Sanfilippo et al., 2021). Similarly high $^{176}Hf/^{177}Hf$ ratios also characterize the Manus Basin, another backarc basin that formed in response to Neogene reversal of subduction polarity between the Pacific and Indian Plates (Figure 7b; Woodhead et al., 2001). That is, the "new mantle" that upwelled between the Pacific and Indian Plates following breakup of the Vitiaz Arc contains an ultra-depleted matrix as its most distinctive feature that is absent from Fiji's breakup basalts only 100 km away.

6.3. Implications for Tectonics

We return now to the question: What caused the Vitiaz Arc to break where it did between Vanuatu and Fiji? Our answer is the subduction of Alexa-type seamounts on the Samoan seamount chain. They were in the right place at the right time (Figures 1 and 2) and have the right isotopic composition (Figures 7–10) to match Fiji's breakup basalts, and the morphology of that part of the Vitiaz Trench Lineament is consistent with seamount subduction (Pelletier & Auzende, 1997).

This question is different from what caused polarity reversal in the Vanuatu and Solomon arcs. That clearly is related to collision with the Ontong Java Plateau (Mann & Taira, 2004). However, it is unknown whether the collision was restricted to the Solomon Islands and led to propagation of polarity reversal southeast toward Fiji, or whether the collision itself extended that far. Although Mann and Taira's Figure 6 infers the latter, we disagree for the tectonic reasons given earlier. Now we add that the isotope systematics of the Fijian breakup basalts, especially their Pb isotope ratios, differ from most Ontong Java lavas. No equivalent geochemical information is available for 12–3 Ma rocks from Vanuatu. Although neither the tectonic nor isotopic arguments against subduction of Ontong Java beneath Vanuatu and Fiji are conclusive, they are internally consistent.

That said, seamount subduction is a common occurrence whereas arc breakup is not. Isotopically similar material seems to be subducting beneath the NMSP without breaking it. Material from the LSC seems to have been subducted beneath the Vitiaz Arc prior to breakup. Slivers from the Hikurangi Plateau seem to have been subducted for several m.y. beneath part of the Kermadec Arc, perhaps contributing to its rifting to create the Havre Trough (Hoernle et al., 2021).

The difference may be like families. As Tolstoy opened Anna Karenina, "All happy families are alike; each unhappy family is unhappy in its own way." In the same way, steady-state subduction is common and fairly well understood by now, but disruptions are not and each one seems different. Collisions can cause subduction to stop or polarities to reverse, arcs can separate along-strike into frontal and remnant parts with a backarc basin in between, or in our case can break across-strike and its parts swing open like saloon doors. It matters whether the causative subducted material is merely OIB-derived volcaniclastic sediment, or small seamounts, or a chain of large guyots and islands, or a Large Igneous Province. It matters how thick and old the subducting lithosphere is. It matters what the convergence angle and rate are. It matters what is on the upper plate.

In the oceanic Vitiaz Arc case, the Ontong Java Plateau collided with the Solomon Island segment of the arc at an oblique angle and slow rate, resulting in prolonged "soft docking" and polarity reversal (Mann & Taira, 2004), whereas collision of its twin, the Hikurangi Plateau, with Zealandia did not. We suggest that the polarity reversal propagated southeastward along the Vitiaz Arc Lineament from the Solomon Islands toward Fiji until the cumulative effects of the collision were insufficient to cause reversal. We infer that the highly oblique subduction of the Samoan seamounts pinned the subduction zone enough to stop the propagation and break the arc, thereby opening the North Fiji Basin behind Vanuatu, and accelerating forearc extension north and east of Fiji to become the Lau Basin. They were the straw that broke the arc's back near Fiji, and enough to push open the saloon doors.

Most versions of the tectonic history shown in Figure 2 infer spreading to form oceanic crust northeast of Vanuatu prior to rotation of Fiji, based on interpretations of Malahoff, Feden, et al.'s (1982) aeromagnetic anomalies. No remnant of the Vitiaz Arc has ever been found along the western Vitiaz Arc Lineament. Whatever happened there remains unknown and perhaps without precedent, but it does not affect our interpretation of Fijian volcanism. We infer slow rifting and rotation of Fiji away from the former plate boundary after Colo plutonism (~7 Ma), starting with the Cikobia boninitic and tholeiitic lavas, and lasting until the start of Fijian OIB volcanism (~3 Ma). Rapid spreading commenced in both the central North Fiji and Lau Basins after that, and evidence of significant slab components in Fijian and Lau Basin magmas disappeared within a few hundred thousand years at that time.

We propose that the new "Indian"-type of mantle consists of a mixture of ultra-depleted matrix with high $^{176}Hf/^{177}Hf$, low $^{206}Pb/^{204}Pb$, and high $\Delta^{208}Pb$, plus diverse kinds of enriched pods. Some of this new mantle appeared in the source of basalts adjacent to the edge of the broken arc immediately south of Viti Levu (i.e., in Vatulele) as early as 4.7 Ma, but it was uncommon in Fiji until ~3 Ma. Many authors have speculated that it came from beneath the Pacific Plate north of the Vitiaz Trench Lineament or Samoa, and that the enriched components melted out preferentially as the mantle advected southward (e.g., Pearce et al., 2007; A. A. Price et al., 2017). Effects attributed to Samoa are restricted to the northeast Lau Basin (Lupton et al., 2015; A. A. Price et al., 2014), but numerical models of the Ontong Java collision predict that toroidal flow around the edge of the broken slab may entrain mantle from beneath the Pacific Plate into the North Fiji Basin (Almeida et al., 2022; Wang et al., 2022). Basalts from the new depleted and enriched mantle are juxtaposed at the Fiji Triple Junction and along the N160° ridge segment north of it (see Figure 1). Although evidence of ultra-depleted mantle has not yet been found in the Ellice Basin, Ontong Java volcanism ~120 Ma left extensive residues of high degrees of melting in the garnet stability field (Tejada et al., 2004). That combination can increase $^{176}Hf/^{177}Hf$ relative to $^{143}Nd/^{144}Nd$ in the residues (e.g., Salters et al., 2011). Therefore, ultra-depleted mantle from the root of the Ontong Java Plateau may be part of what advected into the northern North Fiji ± Lau Basins after breakup of the Vitiaz Arc, rather than subduction of the Plateau itself causing the breakup. Or perhaps some of the depleted and enriched components in the northern North Fiji Basin came from the roots of the Samoan chain (A. A. Price et al., 2022, 2017).

6.4. Implications for Shoshonite Genesis

Shoshonites are exotic arc volcanic rocks rich in K and other large ion lithophile elements. The genesis of the Fijian ones has been explained before (Gill & Whelan, 1989a; Leslie et al., 2009; Rogers & Settlefield, 1994; G.-Z. Sun et al., 2017) and our data mostly confirm their interpretations. That is, shoshonites are small degree melts of depleted mantle in the spinel stability field that was fluxed by a slab-derived fluid or melt. Our isotope data confirm that the ambient mantle to which the slab component was added was similar both to the source of coeval medium- and high-K magmas, and to earlier Fijian volcanic and plutonic rocks. Only the Vatulele shoshonite source included some new, more "Indian-type" mantle. Leslie et al. (2009) attributed most of the differences between Fijian shoshonites to variable fertility of the ambient mantle, whereas we suggest variable *types* of ambient mantle in addition to variable degrees of mantle melting and additions of a slab component.

Our new isotope data reveal that the slab component for both the shoshonitic and high-K rocks was a silicate melt, not just dilute hydrous fluid, because it transported slab-derived LREE including Nd. Consequently, the slab surface temperature was higher than during the steady-state subduction that preceded breakup, and in modern central Tonga (Hergt & Woodhead, 2007). However, the temperature was lower than for the shoshonitic slab component that transported more Hf, Zr, and LREE in the NMSP.

Our trace element data add a few subtleties that confirm the relative importance of recycled OIB-type sediment in the source of the breakup basalts, especially the shoshonites. Th/La ratios of the shoshonites are the same (0.10–0.15) as in the OIB-type volcaniclastics of DSDP Site 204, are as low as at the modern Tongan volcanic front, and are lower than at the Kermadec front (0.15–0.20) despite the much higher Th and La contents in the shoshonites. Hergt and Woodhead (2007) also realized the need for volcaniclastic sediment in the source of Lau Ridge magmas, and their arguments apply even more to the shoshonites farther west. In contrast, the higher Th/La ratios in most Northern Mariana (0.15–0.30) and South Fiji Basin (0.3–0.5) shoshonites, presumably are because of more continentally derived sediment in their sources. That is consistent with both of them having higher $\Delta^{207,208}Pb$ than the Fijian shoshonites. The higher Sr/Ba ratios in Fijian shoshonites (1–3; and 1.5–2.0 just

in Viti Levu) than in the Northern Mariana and South Fiji Basin suites (0.3–1.0) also are consistent with less recycling of continental material in Fiji, and may indicate carbonate in the Fijian source. The slab melt in Fijian shoshonites seems to have been low-temperature and zircon-saturated because their Sm/Hf ratios are >2 which is even higher than in the Northern Marianas shoshonites for which zircon saturation was first invoked (Tollstrup & Gill, 2005). The large enrichments of K, Rb, Ba, and Sr relative to LREE (Figure 6) preclude residual phlogopite (e.g., Condamine et al., 2022). Other than that, the slab component in the shoshonites is not distinctive.

7. Conclusions

1. Comprehensive whole rock analyses are provided for the first time for five volcanoes on Viti Levu and 13 other islands in Fiji that are 3–7 Ma, and include boninitic, low-K, medium-K, high-K, and shoshonitic suites. Collectively we call them "breakup basalts", and we refer to the former arc that they came from as the Vitiaz Arc.
2. The Sr-Pb ± Nd isotope ratios of breakup basalts are most similar to those of the depleted Alexa-type seamounts at the currently known western extent of the Samoan chain. Other seamounts of this chain may already have been subducted at the Vitiaz Trench farther to the west.
3. Because of this isotopic similarity, and because Alexa-type seamounts were on the subducting plate and close to the plate boundary where and when the arc broke, we infer that their subduction contributed to breakup by "pinning" the system enough to block polarity reversal further east. However, the Vitiaz Arc was primed for breakup by the earlier collision of the Ontong Java Plateau with the Solomon Islands sector, and the ensuing propagation of arc polarity reversal along Vanuatu toward Fiji.
4. Breakup of the Vitiaz Arc opened saloon doors to a new and isotopically distinctive mantle whose depleted component is characterized by high $^{176}Hf/^{177}Hf$ and $\Delta^{208}Pb$ ("Indian"-type), and whose enriched components range from like those of Ontong Java to Samoan. It seems to originate beneath the Pacific Plate, and rapidly replaced the old "Pacific"-type mantle that may have contained a slab component derived in part from volcaniclastic sediment or basalt from the LSC.
5. The old "Pacific"-type ambient mantle ± subducted Louisville-type material were important sources for the arc in the Oligocene to Miocene, subducted Alexa-type material became increasingly important in the Pliocene close to the breakup site, and the new "Indian"-type ambient mantle quickly flooded the area after 3 Ma.
6. Breakup started with eruption of boninitic rocks that are similar in composition and pre-breakup location to those erupted later at the northern termination of the Tongan Ridge.
7. The shoshonites represent small degree mantle melts fluxed by slab melts. Only those from Vatulele involved some of the new mantle.

Data Availability Statement

All data for this paper are included in Table 1. Additional analyses from the same volcanoes, and from additional coeval volcanoes, are available at Gill (2020): Compilation of whole rock geochemistry and petrography of samples from the Fiji Islands, Version 1.0. Interdisciplinary Earth Data Alliance (IEDA). https://doi.org/10.26022/IEDA/111498 Hand specimens of most of the samples in this study, and other well-analyzed ones from the ECL, are available from the US Museum of Natural History (Smithsonian) except for those with a 68-, 69-, or C prefix, for which agate-ground powders are available from the first author. Any use of trade, firm, or product names is for descriptive purposes only and does not imply endorsement by the US Government.

Acknowledgments
This paper is indebted to the late Peter Whelan and Jon Stoen who collected and made the initial analyses of these samples, and who financed those activities, respectively, as part of oil and mineral exploration in Fiji in the 1980s. Peter Rodda, Frank Coulson, Derek Woodhall, and Bill Hindle of the Fiji Mineral Resources Department did the underlying geological mapping and advised about the sampling; Rodda and Woodhall provided several samples; Bob Duncan measured the K-Ar age of C48 in 1985; and Simon Jackson made two ICPMS analyses in 1993. Julian Pearce and Pam Kempton analyzed some of the samples as an adjunct to the Pearce et al. (2007) paper. Ina Simon prepared some of the samples at GEOMAR where Silke Hauff and Karin Junge helped with the isotope chemistry and TIMS analyses while Marcus Gutjahr carried out the Hf isotope analysis. Nick Mortimer, Brian Taylor, and the late Jasper Konter provided helpful background about regional tectonics. Maria Tejada graciously shared the as-measured isotope data for Ontong Java basalts. We thank Matt Loewen, Allen Stork, editor Marie Edmonds, and an anonymous reviewer for careful reading of the manuscript. MGJ acknowledges support from NSF OCE-1929095.

References

Almeida, J., Riel, N., Rosas, F. M., Duarte, J. C., & Schellart, W. P. (2022). Polarity-reversal subduction zone initiation triggered by buoyant plateau obstruction. *Earth and Planetary Science Letters*, *577*, 117195. https://doi.org/10.1016/j.epsl.2021.117195

Auzende, J.-M., Pelletier, B., & Eissen, J.-P. (1995). The North Fiji Basin geology, structure, and geodynamic evolution. In B. Taylor (Ed.), *Back-arc basins: Tectonics and magmatism* (pp. 139–175). Plenum Press. https://doi.org/10.1007/978-1-4615-1843-3_4

Auzende, J.-M., Pelletier, B., & Lajoy, Y. (1994). Twin active spreading centers in the North Fiji Basin. *Geology*, *22*, 63–66. https://doi.org/10.1130/0091-7613(1994)022<0063:tasrit>2.3.co;2

Beier, C., Vanderkluysen, L., Regelous, M., Mahoney, J. J., & Garbe-Schonberg, D. (2011). Lithospheric control on geochemical composition along the Louisville Seamount Chain. *Geochemistry, Geophysics, Geosystems*, *12*(9). https://doi.org/10.1029/2011GC003690

Benyshek, E., Wessel, P., & Taylor, B. (2019). Tectonic reconstruction of the Ellice Basin. *Tectonics*, *38*, 3854–3865. https://doi.org/10.1029/2019TC005650

Billen, M., & Stock, J. (2000). Morphology and origin of the Osbourn Trough. *Journal of Geophysical Research*, *105*(B6), 13481–13489. https://doi.org/10.1029/2000jb900035

Bloomer, S. H., Stern, R. J., Fisk, E., & Geschwind, C. H. (1989). Shoshonitic volcanism in the Northern Mariana and Volcano Arc 1. Mineralogic and major and trace element characteristics. *Journal of Geophysical Research*, *94*, 4469–4496. https://doi.org/10.1029/jb094ib04p04469

Brocher, T. M. (1985). On the formation of the Vitiaz Trench Lineament and North Fiji Basin. *Geological Investigations of the Northern Melanesian Borderland, Circum-Pacific Council for Energy and Mineral Resources Earth Science Series* (Vol. *4*, pp. 13–33).

Buff, L., Jackson, M. G., Konrad, K., Konter, J. G., Bizimis, M., Price, A., et al. (2021). Missing links" for the long-lived Macdonald and Arago hotspots, South Pacific Ocean. *Geology*, *49*, 541–544. https://doi.org/10.1130/g48276.1

Carney, J. N., Macfarlane, A., & Mallick, D. I. J. (1985). The Vanuatu Island Arc—An outline of stratigraphy, structure, and petrology. In A. E. M. Nairn, F. G. Stehli, & S. Uyeda (Eds.), *The ocean basins and margins, The Pacific Ocean* (Vol. 7A, pp. 683–718). Plenum Press. https://doi.org/10.1007/978-1-4613-2351-8_14

Castillo, P. R., Lonsdale, P. F., Moran, C. L., & Hawkins, J. W. (2009). Geochemistry of mid-Cretaceous Pacific crust being subducted along the Tonga-Kermadec Trench: Implications for the generation of arc lavas. *Lithos*, *112*, 87–102. https://doi.org/10.1016/j.lithos.2009.03.041

Chase, C. G. (1971). Tectonic history of the Fiji Plateau. *The Geological Society of America Bulletin*, *82*, 3087–3110. https://doi.org/10.1130/0016-7606(1971)82[3087:thotfp]2.0.co;2

Chen, J., Chen, Y. J., Wiens, D. A., Wie, S. S., Zha, Y., Julia, J., & Gai, C. (2019). Crustal and lithospheric structure of inactive volcanic arc terrains in Fiji. *Tectonophysics*, *750*, 394–403. https://doi.org/10.1016/j.tecto.2018.07.014

Class, C., & Lehnert, K. (2012). *PetDB expert MORB compilation, Version 1.0*. Interdisciplinary Earth Data Alliance (IEDA). https://doi.org/10.1594/IEDA/100060

Cole, J. W., Gill, J. B., & Woodhall, D. (1985). Petrologic history of the Lau Ridge, Fiji. In D. W. Scholl, & T. L. Vallier (Eds.), *Geology and offshore resources of Pacific Island Arcs; Tonga region* (Vol. 2, pp. 379–414). Circum-Pacific Council Energy and Minerals Resources.

Cole, J. W., Graham, I. J., & Gibson, I. L. (1990). Magmatic evolution of Late Cenozoic volcanic rocks of the Lau Ridge, Fiji. *Contributions to Mineralogy and Petrology*, *104*, 540–554. https://doi.org/10.1007/bf00306663

Condamine, P., Couzinie, S., Fabbrizio, A., Devidal, J.-L., & Medard, E. (2022). Trace element partitioning during incipient melting of phlogopite-peridotite in the spinel and garnet stability fields. *Geochimica et Cosmochimica Acta*, *327*, 53–78. https://doi.org/10.1016/j.gca.2022.04.011

Coulson, F. I. E. (1971). Geology of western Vanua Levu. *Bulletin Geological Survey Department Suva Fiji*, *17*.

Couslon, F. I. E. (1976). Geology of the Lomaiviti and Moala Island Groups. *Bulletin Mineral Resources Division Fiji Bulletin*, *2*.

Crawford, W. C., Hildebrand, J. A., Dorman, L. M., Webb, S. C., & Wiens, D. A. (2003). Tonga Ridge and Lau Basin crustal structure from seismic refraction data. *Journal of Geophysical Research*, *108*(B4). https://doi.org/10.1029/2001JB001435

Cronan, D. S., & Hodkinson, R. A. (1997). Geochemistry of hydrothermal sediments from ODP Sites 834 and 835 in the Lau Basin, southwest Pacific. *Marine Geology*, *14*, 237–268. https://doi.org/10.1016/s0025-3227(97)00071-6

Danyushevsky, L. V., Falloon, T. J., Crawford, A. J., Tetroeva, S. A., Leslie, R. A., & Verbeteen, A. C. (2008). High-Mg adakites from Kadavu Group, Fiji: Evidence for the mantle origin of adakite parental melts. *Geology*, *36*(6), 499–502. https://doi.org/10.1130/G24349A.1

Davy, B., Hoernle, K., & Werner, R. (2008). Hikurangi Plateau: Crustal structure, rifted formation, and Gondwana subduction history. *Geochemistry, Geophysics, Geosystems*, *9*, Q07004. https://doi.org/10.1029/2007GC001855

Elburg, M. A., Foden, J. D., van Bergen, M. J., & Zulkarain, I. (2005). Australia and Indonesia in collision: Geochemical sources of magmatism. *Journal of Volcanology and Geothermal Research*, *140*, 25–47. https://doi.org/10.1016/j.jvolgeores.2004.07.014

Falloon, T. J., Danyushevsky, L., Crawford, A. J., Meffre, S., Woodhead, J. D., & Bloomer, S. H. (2008). Boninites and adakites from the northern termination of the Tonga Trench: Implications for adakite petrogenesis. *Journal of Petrology*, *49*, 697–715. https://doi.org/10.1093/petrology/egn009

Falvey, D. A. (1978). Analysis of paleomagnetic data from the New Hebrides. *Bulletin of the Australian Society of Exploration Geophysicists*, *9*, 117–123. https://doi.org/10.1071/eg978117

Finlayson, V. A., Konter, J. G., Konrad, K., Koppers, A. A. P., Jackson, M., & Rooney, T. O. (2018). Sr-Pb-Nd-Hf isotopes and $^{40}Ar/^{39}Ar$ ages reveal a Hawaii-Emperor-style bend in the Rurutu hotspot. *Earth and Planetary Science Letters*, *500*, 168–179. https://doi.org/10.1016/j.epsl.2018.08.020

Fryer, P., Gill, J. B., & Jackson, M. C. (1997). Volcanologic and tectonic evolution of the Kasuga seamounts, northern Mariana Trough: ALVIN submersible investigations. *Journal of Volcanology and Geothermal Research*, *79*, 277–311. https://doi.org/10.1016/s0377-0273(97)00013-9

Gill, J. B. (1970). Geochemistry of Viti Levu, Fiji, and its evolution as an island arc. *Contributions to Mineralogy and Petrology*, *27*, 179–203. https://doi.org/10.1007/bf00385777

Gill, J. B. (1972). *The geochemical evolution of Fiji*. Australian Nation University Ph.D.

Gill, J. B. (1976). Composition and age of Lau Basin and Ridge volcanic rocks: Implications for evolution of an interarc basin and remnant arc. *The Geological Society of America Bulletin*, *87*, 1384–1395. https://doi.org/10.1130/0016-7606(1976)87<1384:caaolb>2.0.co;2

Gill, J. B. (1981). *Orogenic andesites and plate tectonics* (p. 390). Springer-Verlag.

Gill, J. B. (1984). Sr-Pb-Nd isotopic evidence that both MORB and OIB sources contribute to oceanic island arc magmas in Fiji. *Earth and Planetary Science Letters*, *68*, 443–458. https://doi.org/10.1016/0012-821x(84)90129-8

Gill, J. B. (1987). Early geochemical evolution of an oceanic island arc and backarc: Fiji and the South Fiji Basin. *The Journal of Geology*, *95*, 589–615. https://doi.org/10.1086/629158

Gill, J. B. (2020). *Compilation of whole rock geochemistry and petrography of samples from the Fiji Islands, Version 1.0*. Interdisciplinary Earth Data Alliance (IEDA). https://doi.org/10.26022/IEDA/111498

Gill, J. B., & Gorton, M. (1973). A proposed geological and geochemical history of eastern Melanesia. In P. Coleman (Ed.), *The western Pacific island arcs marginal seas geochemistry* (pp. 543–566). University of Western Australia Press.

Gill, J. B., & Stork, A. L. (1979). Miocene low-K dacites and Trondhjemites of Fiji. In *Miocene Low-K Dacites and Trondhjemites of Fiji, Trondhjemites, Dacites, and Related Rocks* (pp. 629–649). Elsevier Scientific Publishing Company. https://doi.org/10.1016/b978-0-444-41765-7.50027-7

Gill, J. B., & Whelan, P. M. (1989a). Early rifting of an oceanic island arc (Fiji) produced shoshonitic to medium-K basalts. *Journal of Geophysical Research*, *94*, 4561–4578. https://doi.org/10.1029/jb094ib04p04561

Gill, J. B., & Whelan, P. M. (1989b). Postsubduction ocean island alkali basalts in Fiji. *Journal of Geophysical Research*, *94*, 4579–4588. https://doi.org/10.1029/jb094ib04p04579

Gill, J. B., Hoernle, K., Todd, E., Hauff, F., Werner, R., Timm, C., et al. (2021). Basalt geochemistry and mantle flow during early backarc basin evolution: Havre Trough and Kermadec Arc, southwest Pacific. *Geochemistry, Geophysics, Geosystems*, *22*, e2020GC009339. https://doi.org/10.1029/2020gc009339

Gill, J. B., Stork, A. L., & Whelan, P. M. (1984). Volcanism accompanying backarc basin development in the southwest Pacific. *Tectonophysics*, *102*, 207–224. https://doi.org/10.1016/0040-1951(84)90014-3

Green, T. H., & Ringwood, A. E. (1968). Genesis of the calc-alkaline igneous rock suite. *Contributions to Mineralogy and Petrology*, *18*, 105–162. https://doi.org/10.1007/bf00371806

Gribble, R. F., Stern, R. J., Newman, S., Bloomer, S. H., & O'Hearn, T. (1998). Chemical and isotopic composition of lavas from the Northern Mariana Trough: Implications for magmagenesis in backarc basins. *Journal of Petrology*, *39*, 125–154. https://doi.org/10.1093/petroj/39.1.125

Grzesczyk, A., Lefevre, C., Monzier, M., Eissen, J.-P., Dupont, J., & Maillet, P. (1991). Mise en evidence d'un volcanisme transitionnel Pliocene superieur sur Futuna et Alofi (SE Pacifiique): Un nouveau temoin de l'evolution geodynamoque nord-Tonga. *Comptes Rendus de l'Académie des Sciences, Série II* (Vol. *312*, pp. 713–720).

Gutscher, M.-A., Spakman, W., Bijwaard, H., & Engdahl, E. R. (2000). Geodynamics of flat subduction: Seismicity and tomographic constraints from the Andean margin. *Tectonics*, *19*, 814–833. https://doi.org/10.1029/1999tc001152

Hanyu, T., Gill, J. B., Tatsumi, Y., Kimura, J.-I., Sato, K., Chang, Q., et al. (2012). Across- and along-arc geochemical variations of lava chemistry in the Sangihe arc: Various fluid and melt slab fluxes in response to slab temperature. *Geochemistry, Geophysics, Geosystems*, *13*(1). 10.1029/2012GC004346

Hart, S. R. (1984). A large-scale isotope anomaly in the Southern Hemisphere. *Nature*, *309*, 753–757. https://doi.org/10.1038/309753a0

Hart, S. R., Coetzee, M., Workman, R. K., Blusztajn, J., Johnson, K. T. M., Sinton, J. M., et al. (2004). Genesis of the Western Samoa seamount province: Age, geochemical fingerprint and tectonics. *Earth and Planetary Science Letters*, *227*, 37–56. https://doi.org/10.1016/j.epsl.2004.08.005

Hathway, R., & Colley, H. (1994). Eocene to Miocene geology of southwest Viti Levu, Fiji. In A. J. Stevenson, R. H. Herzer, & P. F. Ballance (Eds.), *Geology and submarine resources of the Tonga-Kau-Fiji Region* (Vol. 8, pp. 153–169). SOPAC Technical Bulletin.

Hauff, F., Hoernle, K., Gill, J., Werner, R., Timm, C., Garbe-Schönberg, D., et al. (2021). R/V SONNE Cruise SO255 "VITIAZ": An integrated major element, trace element, and Sr-Nd-Pb-Hf isotope data set of volcanic rocks from the Colville and Kermadec Ridges, the Quaternary Kermadec volcanic front and the Havre Trough backarc basin (Version 1.0): Interdisciplinary Earth Data Alliance (IEDA). https://doi.org/10.26022/IEDA/111723

Hergt, J. M., & Farley, K. N. (1994). Major element, trace element, and isotope (Pb, Sr, and Nd) variations in Site 834 basalts: Implications for the initiation of backarc opening. In J. W. Hawkins, et al. (Eds.), *Proceedings of the Ocean Drilling Program, Scientific Results, Lau Basin*. Ocean Drilling Program (pp. 471–485). https://doi.org/10.2973/odp.proc.sr.135.144.1994

Hergt, J. M., & Hawkesworth, C. J. (1994). Pb-, Sr-, and Nd-isotopic evolution of the Lau Basin; implications for mantle dynamics during backarc opening. In J. W. Hawkins, et al. (Eds.), *Proceedings of the Ocean Drilling Program, Scientific Results, Lau Basin*. Ocean Drilling Program (pp. 505–517). https://doi.org/10.2973/odp.proc.sr.135.142.1994

Hergt, J. M., & Woodhead, J. D. (2007). A critical evaluation of recent models for Lau-Tonga arc-backarc basin magmatic evolution. *Chemical Geology*, *245*, 9–44. https://doi.org/10.1016/j.chemgeo.2007.07.022

Herzer, R. H., Barker, D. H. N., Roest, W. R., & Mortimer, N. (2011). Oligocene-Miocene spreading history of the northern South Fiji Basin and implications for the evolution of the New Zealand plate boundary. *Geochemistry, Geophysics, Geosystems*, *12*(2). https://doi.org/10.1029/2010gc003291

Hoernle, K., Gill, J. B., Timm, C., Hauff, F., Werner, R., Garbe-Schonberg, D., & Gutjahr, M. (2021). Hikurangi Plateau subduction a trigger for Vitiaz arc splitting and Havre Trough opening (southwestern Pacific). *Geology*, *49*, 536–540. https://doi.org/10.1130/g48436.1

Ibbotson, P. (1967). *Petrology of the Tertiary caldera, Tavua goldfield*. Fiji Geological Survey Department Memoir (Vol. 3).

Ishizuka, O., Hickey-Vargas, R., Arculus, R. J., Yogodzinski, G. M., Savov, I. P., Kusano, Y., et al. (2018). Age of Izu-Bonin-Mariana arc basement. *Earth and Planetary Science Letters*, *481*, 80–90. https://doi.org/10.1016/j.epsl.2017.10.023

Jackson, M. G., Halldorsson, S. A., Price, A., Kurz, M. D., Konter, J. G., Koppers, A. A. P., & Day, J. M. D. (2020). Contrasting old and young volcanism from the Aitutaki, Cook Islands: Implications for the origins of the Cook-Austral volcanic chain. *Journal of Petrology*, *61*(3). https://doi.org/10.1093/petrology/egaa037

Jackson, M. G., Hart, S. R., Konter, J. G., Koppers, A. A. P., Staudigel, H., Kurz, M. D., et al. (2010). Samoan hot spot track on a "hot spot highway": Implications for mantle plumes and a deep Samoan mantle source. *Geochemistry, Geophysics, Geosystems*, *11*(1). 10.1029/2010GC003232

Jackson, M. G., Kurz, M. D., Hart, S. R., & Workman, R. K. (2007). New Samoan lavas from Ofu Island reveal a hemispherically heterogeneous high $^{3}He/^{4}He$ mantle. *Earth and Planetary Science Letters*, *264*, 360–374. https://doi.org/10.1016/j.epsl.2007.09.023

Jenner, G. A., Longerich, H. P., Jackson, S. E., & Fryer, B. J. (1990). ICP-MS: A powerful tool for high-precision trace element analysis in Earth sciences: Evidence from analysis of selected U.S.G.S. reference samples. *Chemical Geology*, *83*, 133–148. https://doi.org/10.1016/0009-2541(90)90145-w

Jezek, P. A., Bryan, W. B., Haggerty, S. E., & Johnson, H. P. (1977). Petrography, petrology, and tectonic implications of Mitre Island, northern Fiji Plateau. *Marine geology*, *24*, 123–148. https://doi.org/10.1016/0025-3227(77)90005-6

Leslie, R. A. J., Danyushevsky, L. V., Crawford, A. J., & Verbeeten, A. C. (2009). Primitive shoshonites from Fiji: Geochemistry and source components. *Geochemistry, Geophysics, Geosystems*, *10*(7). https://doi.org/10.1029/2008gc002326

Lupton, J., Rubin, K. H., Arculus, R., Lilley, M., Butterfield, D., Resing, J., et al. (2015). Helium isotope, $C/^{3}He$, and Ba-Nb-Ti signatures in the northern Lau Basin: Distinguishing arc, backarc, and hotspot affinities. *Geochemistry, Geophysics, Geosystems*, *16*, 1133–1155. https://doi.org/10.1002/2014GC005625

Madson, J. K., Thorkelson, D. J., Friedman, R. M., & Marshall, D. D. (2006). Cenozoic to Recent plate configurations in the Pacific Basin: Ridge subduction and slab window magmatism in western North America. *Geosphere*, *2*(1), 11–34. https://doi.org/10.1130/GES00020.1

Malahoff, A., Feden, R. H., & Fleming, H. S. (1982). Magnetic anomalies and tectonic fabric of marginal basins north of New Zealand. *Journal of Geophysical Research*, *87*, 4109–4125. https://doi.org/10.1029/jb087ib05p04109

Malahoff, A., Hammond, S. R., Naughton, J. J., Keeling, D. L., & Richmond, R. N. (1982). Geophysical evidence for post-Miocene rotation of Viti Levu, Fiji, and its relationship to the tectonic development of the North Fiji Basin. *Earth and Planetary Science Letters*, *57*, 398–414. https://doi.org/10.1016/0012-821x(82)90159-5

Mann, P., & Taira, A. (2004). Global tectonic significance of the Solomon Islands and Ontong Java Plateau convergent zone. *Tectonophysics*, *389*, 137–190. https://doi.org/10.1016/j.tecto.2003.10.024

Marien, C. S., Drewes-Todd, E. K., Stork, A., Todd, E., Gill, J. B., Hoffmann, J. E., et al. (2022). Juvenile continental crust evolution in a modern oceanic arc setting: Petrogenesis of Cenozoic felsic plutons in Fiji, SW Pacific. *Geochimica et Cosmochimica Acta*, *320*, 339–365. https://doi.org/10.1016/j.gca.2021.11.033

Martin, A. K. (2013). Double-saloon-door tectonics in the North Fiji Basin. *Earth and Planetary Science Letters*, *374*, 191–203. https://doi.org/10.1016/j.epsl.2013.05.041

Mortimer, N., Bosch, D., Laporte-Magoni, C., Todd, E., & Gill, J. B. (2021). Sr, Nd, Hf, and Pb isotope geochemistry of Early Miocene shoshonitic lavas from the South Fiji Basin. *New Zealand Journal of Geology and Geophysics*, *65*, 374–379. https://doi.org/10.1080/00288306.2021.1876110

Musgrave, R. J., & Firth, J. V. (1999). Magnitude and timing of New Hebrides Arc rotation: Paleomagnetic evidence from Nendo, Solomon Islands. *Journal of Geophysical Research*, *104*, 2841–2853. https://doi.org/10.1029/1998jb900080

Nakamura, N. (1974). Determination of REE, Ba, Fe, Mg, Na, and K in carbonaceous and ordinary chondrites. *Geochimica et Cosmochimica Acta*, *38*, 757–775. https://doi.org/10.1016/0016-7037(74)90149-5

Niu, Y., Regelous, M., Wendt, I. J., Batiza, R., & O'Hara, M. J. (2002). Geochemistry of near-EPR seamounts: Importance of source vs. process and the origin of enriched mantle component. *Earth and Planetary Science Letters*, *199*, 327–345. https://doi.org/10.1016/s0012-821x(02)00591-5

Orovan, E. A., Cooke, D. R., Harris, A. C., Ackerman, B., & Lawlis, E. (2018). Geology and isotope geochemistry of the Wainaulo Cu-Au porphyry deposit, Namosi District, Fiji. *Econonmic Geology*, *113*, 133–161. https://doi.org/10.5382/econgeo.2018.4546

Packham, G. H. (1973). A speculative Phanerozoic history of the South-west Pacific. In P. Coleman (Ed.), *The western Pacific island arcs marginal seas geochemistry* (pp. 369–388). University of Western Australia Press.

Packham, H. H. (1982). Forward to papers on the tectonics of the southwest Pacific region. *Tectonophysics*, *87*, 1–10. https://doi.org/10.1016/0040-1951(82)90217-7

Pearce, J. A., Kempton, P. D., & Gill, J. B. (2007). Hf-Nd evidence for the origin and distribution of mantle domains in the SW Pacific. *Earth and Planetary Science Letters*, *260*, 98–114. https://doi.org/10.1016/j.epsl.2007.05.023

Pearce, J. A., Kempton, P. D., Nowell, G. M., & Noble, S. R. (1999). Hf-Nd element and isotope perspective on the nature and provenance of mantle and subduction components in western Pacific arc-basin systems. *Journal of Petrology*, *40*, 1579–1611. https://doi.org/10.1093/petroj/40.11.1579

Pearce, J. A., Stern, R. J., Bloomer, S. H., & Fryer, P. (2005). Geochemical mapping of the Mariana arc-basin system: Implications for the nature and distribution of subduction components. *Geochemistry, Geophysics, Geosystems*, *6*(7). https://doi.org/10.1029/2004gc000895

Peate, D. W., & Pearce, J. A. (1998). Causes of spatial compositional variations in Mariana arc lavas: Trace element evidence. *Island Arc*, *7*, 479–495. https://doi.org/10.1111/j.1440-1738.1998.00205.x

Pelletier, B., & Auzende, J.-M. (1996). Geometry and structure of the Vitiaz Trench Lineament (SW Pacific). *Marine Geophysical Researches*, *18*, 305–335. https://doi.org/10.1007/bf00286083

Pelletier, B., Lafoy, Y., & Missegue, F. (1993). Morphostructure and magnetic fabric of the northwest North Fiji Basin. *Geophysical Research Letters*, *20*, 1151–1154. https://doi.org/10.1029/93gl01240

Pelletier, B., Lagabrielle, Y., Benoit, M., Cabioch, G., Calmant, S., Garel, E., & Guivel, C. (2001). Newly identified segments of the Pacific-Australia plate boundary along the North Fiji transform zone. *Earth and Planetary Science Letters*, *193*, 347–358. https://doi.org/10.1016/s0012-821x(01)00522-2

Plank, T. (2005). Constraints from Thorium/Lanthanum on sediment recycling at subduction zones and the evolution of continents. *Journal of Petrology*, *46*, 921–944. https://doi.org/10.1093/petrology/egi005

Price, A. A., Jackson, M. G., Blichert-Toft, J., Blusztajn, J., Conatser, C. S., Konter, J. G., et al. (2016). Geochemical evidence in the northeast Lau Basin for subduction of the Cook-Austral volcanic chain in the Tonga Trench. *Geochemistry, Geophysics, Geosystems*, *17*, 1694–1724. https://doi.org/10.1002/2015GC006237

Price, A. A., Jackson, M. G., Blichert-Toft, J., Hall, P. S., Sinton, J. M., Kurz, M. D., & Blusztajn, J. (2014). Evidence for a broadly distributed Samoan-plume signature in the northern Lau and North Fiji Basins. *Geochemistry, Geophysics, Geosystems*, *15*, 986–1008. https://doi.org/10.1002/2013gc005061

Price, A. A., Jackson, M. G., Blichert-Toft, J., Konrad, K., Bizimis, M., Koppers, A., et al. (2022). Samoan-like EM1 rejuvenated volcanism on a HIMU Cook-Austral volcano: Contrasting volcanism on a single "hotspot highway" volcano at Papatua Seamount, American Samoa. *Journal of Petrology*. (in press).

Price, A. A., Jackson, M. G., Blichert-Toft, J., Kurz, M. D., Gill, J., Blusztajn, J., et al. (2017). Geodynamic implications for zonal and meridional isotopic patterns across the northern Lau and North Fiji Basins. *Geochemistry, Geophysics, Geosystems*, *18*, 1013–1042. https://doi.org/10.1002/2016GC006651

Price, R. C., Maillet, P., McDougall, I., & Dupont, J. (1991). The geochemistry of basalts from the Wallis Islands, Northern Melanesian Borderland: Evidence for a lithospheric origin for Samoan-type basaltic magmas. *Journal of Volcanology and Geothermal Research*, *45*, 267–288. https://doi.org/10.1016/0377-0273(91)90063-6

Pysklywec, R. N., Mitrovica, J. X., & Ishii, M. (2003). Mantle avalanche as a driving force for tectonic reorganization in the southwest Pacific. *Earth and Planetary Science Letters*, *209*, 29–38. https://doi.org/10.1016/s0012-821x(03)00073-6

Reagan, M. K., Heaton, D. E., Schmitz, M. D., Pearce, J. A., Shervais, J. W., & Koppers, A. A. P. (2019). Forearc ages reveal extensive short-lived and rapid seafloor spreading following subduction initiation. *Earth and Planetary Science Letters*, *506*, 520–529. https://doi.org/10.1016/j.epsl.2018.11.020.epsl.2018.11.020

Reyners, M., Eberhart-Phillips, D., & Bannister, S. (2011). Tracking repeated subduction of the Hikurangi Plateau beneath New Zealand. *Earth and Planetary Science Letters*, *311*, 165–171. https://doi.org/10.1016/j.epsl.2011.09.011

Rickard, M. (1966). Reconnaissance geology of Vanua Levu. *Fiji Mineral Resources Division Memoir*.

Rodda, P. (1976). Geology of northern and central Viti Levu. *Fiji Mineral Resources Division Bulletin* (Vol. *3*).

Rogers, N. W., & Settlefield, T. N. (1994). Potassium and incompatible-element enrichment in shoshonitic lavas from Tavua volcano, Fiji. *Chemical Geology*, *118*, 43–62. https://doi.org/10.1016/0009-2541(94)90169-4

Ruellan, E., Delteil, J., Wright, I., & Matsumoto, T. (2003). From rifting to active spreading in the Lau Basin-Havre Trough backarc system (SW Pacific): Locking/unlocking induced by seamount chain subduction. *Geochemistry, Geophysics, Geosystems*, *4*(5). https://doi.org/10.1029/2001GC000261

Ryder, C. H., Gill, J. B., Tepley, F., Ramos, F., & Reagan, M. (2006). Closed-to open-system differentiation at Arenal Volcano (1968–2003). *Journal of Volcanology and Geothermal Research*, *157*, 75–93. https://doi.org/10.1016/j.jvolgeores.2006.03.046

Salters, V. J. M., Mallick, S., Hart, S. R., Langmuir, C. E., & Stracke, A. (2011). Domains of depleted mantle: New evidence from hafnium and neodymium isotopes. *Geochemistry, Geophysics, Geosystems*, *12*(8). https://doi.org/10.1029/2011GC003617

Sanfilippo, A., Salters, V. J. M., Sokolov, S. Y., Peyve, A. A., & Stracke, A. (2021). Ancient refractory asthenosphere revealed by mantle re-melting at the Arctic Mid-Atlantic Ridge. *Earth and Planetary Science Letters*, *566*, 116981. https://doi.org/10.1016/j.epsl.2021.116981

Schellart, W. P., Lister, G. S., & Toy, V. G. (2006). A Late Cretaceous and Cenozoic reconstruction of the southwest Pacific region: Tectonics controlled by subduction and slab rollback processes. *Earth-Science Reviews*, *76*, 191–233. https://doi.org/10.1016/j.earscirev.2006.01.002

Sdrolias, M., Muller, R. D., & Gaina, C. (2003). Tectonic evolution of the southwest Pacific using constraints from backarc basins. *Geological Society of Australia Special Publication*, *22*, 343–359. https://doi.org/10.1130/0-8137-2372-8.343

Sinton, J. M., Johnson, K. T. M., & Price, R. C. (1985). Geological Investigations of the Northern Melanesian Borderland. In *Circum-Pacific Council for Energy and Mineral Resources Earth Science Series* (Vol. *4*, pp. 34–64).

Spry, P. G., & Scherbarth, N. L. (2006). The gold-vanadium-tellurium association at the Tuvatu gold-silver prospect, Fiji: Conditions of ore deposition. *Mineralogy and Petrology*, *87*, 171–186. https://doi.org/10.1007/s00710-006-0128-6

Stern, R. J., Jackson, M. C., Fryer, P., & Ito, E. (1993). O, Sr, Nd, and Pb isotopic composition of the Kasuga Cross-Chain in the Mariana arc: A new perspective on the K-h relationship. *Earth and Planetary Science Letters*, *119*, 459–475. https://doi.org/10.1016/0012-821x(93)90056-f

Sun, G.-Z., Xu, W.-L., Wang, Z.-W., Guo, P., & Liu, S.-W. (2017). Petrogenesis of Cenozoic shoshonitic rocks in Fiji: Constraints from mineral and whole-rock geochemistry. *Geological Journal*, *53*, 1–2778. https://doi.org/10.1002/gj.3109

Sun, S.-S., & McDonough, W. F. (1989). Chemical and isotopic systematics of oceanic basalts: Implications for mantle composition and processes. *Geological Society Special Publications*, *42*, 313–345. https://doi.org/10.1144/gsl.sp.1989.042.01.19

Tanaka, T., Imai, A., Egashira, S., Sakomoto, S., Yasunaga, K., & Maeda, K. (2010). Petrological and geochemical characteristics of intrusive rocks related to porphyry copper mineralization and the implications for the genesis of deposits in the Namosi area, Viti Levu, Republic of the Fiji Islands. *Resource Geology*, *60*, 35–51. https://doi.org/10.1111/j.1751-3928.2010.00113.x

Taylor, B. (2006). The single largest oceanic plateau: Ontong Java-Manihiki-Hikurangi. *Earth and Planetary Science Letters*, *241*, 372–380. https://doi.org/10.1016/j.epsl.2005.11.049

Taylor, G. K., Gascoyne, J., & Colley, H. (2000). Rapid rotation of Fiji: Paleomagnetic evidence and tectonic implications. *Journal of Geophysical Research*, *105*, 5771–5781. https://doi.org/10.1029/1999jb900305

Taylor, S. R., Capp, A., Graham, A. L., & Blake, D. H. (1967). Trace element abundances in andesite II: Saipan, Bougainville, and Fiji. *Contributions to Mineralogy and Petrology*, *23*, 1–26.

Tejada, M. L. G., Mahoney, J. J., Castillo, P. R., Ingle, S. P., Sheth, H. C., & Weis, D. (2004). Pin-pricking the elephant: Evidence on the origin of the Ontong Java Plateau from Pb-Sr-Hf-Nd isotopic characteristics of ODP Leg 192 basalts. In J. G. Fitton, J. J. Mahoney, P. J. Wallace, & A. D. Saunders (Eds.), *Origin and evolution of the Ontong Java Plateau* (Vol. 229, pp. 133–150). Geological Society Special Publication. https://doi.org/10.1144/gsl.sp.2004.229.01.09

Timm, C., Davy, B., Haase, K., Hoernle, K. A., Graham, I. J., De Ronde, C. E., et al. (2014). Subduction of the oceanic Hikurangi Plateau and its impact on the Kermadec arc. *Nature Communications*, *5*, 29. https://doi.org/10.1038/ncomms5923

Todd, E., Gill, J. B., & Pearce, J. A. (2012). A variably enriched mantle wedge and contrasting melt types during arc stages following initiation in Fiji and Tonga, southwest Pacific. *Earth and Planetary Science Letters*, *335–336*, 180–194. https://doi.org/10.1016/j.epsl.2012.05.006

Todd, E., Gill, J. B., Wysoczanski, R. J., Hergt, J., Wright, I. C., Leybourne, M. I., & Mortimer, N. (2011). Hf isotopic evidence for small-scale heterogeneity in the mode of mantle wedge enrichment: Southern Havre Trough and South Fiji Basin back arcs. *Geochemistry, Geophysics, Geosystems*, *12*(9). https://doi.org/10.1029/2011GC003683

Todd, E., Stork, A., Drewes-Todd, E. K., Tani, K., Allen, C. M., & Gill, J. B. (2021). *Geochemistry and geochronology of Cenozoic plutons of Viti Levu, Fiji, Version 1.0. Interdiscip*. Earth Data Alliance. https://doi.org/10.26022/IEDA/111854

Tollstrup, D. L., & Gill, J. B. (2005). Hafnium systematics of the Mariana arc: Evidence for sediment melt and residual phases. *Geology*, *33*, 737–740. https://doi.org/10.1130/g21639.1

Turner, S. J., & Langmuir, C. H. (2022). Quantitative framework for global variations in arc geochemistry. *Earth and Planetary Science Letters*, *584*, 117411. https://doi.org/10.1016/j.epsl.2022.117411

Turner, S., Hawkesworth, C., Rogers, N., Bartlett, J., Worthington, T., Hergt, J., et al. (1997). ^{238}U-^{230}Th disequilibria, magma petrogenesis, and flux rates beneath the depleted Tonga-Kermadec island arc. *Geochimica et Cosmochimica Acta*, *61*, 4855–4884. https://doi.org/10.1016/s0016-7037(97)00281-0

Vanderkluysen, L., Mahoney, J. J., Koppers, A. A. P., Beier, C., Regelous, M., Gee, J. S., & Lonsdale, P. F. (2014). Louisville Seamount Chain: Petrogenetic processes and geochemical evolution of the mantle source. *Geochemistry, Geophysics, Geosystems*, *15*, 2380–2400. https://doi.org/10.1002/2014gc005288

Vervoort, J. D., & Blichert-Toft, J. (1999). Evolution of the depleted mantle: Hf isotope evidence from juvenile rocks through time. *Geochimica et Cosmochimica Acta*, *63*, 533–556. https://doi.org/10.1016/s0016-7037(98)00274-9

Vogt, P. R. (1973). Subduction and aseismic ridges. *Nature*, *241*, 189–191. https://doi.org/10.1038/241189a0

Wang, L., Dai, L., Gong, W., Li, S., Jiang, X., Foulger, G., et al. (2022). Subduction initiation at the Solomon back-arc basin: Contributions from both island arc rheological strength and oceanic plateau collision. *Geophysical Research Letters*, *49*, e2021GL097666. https://doi.org/10.1029/2021gl097666

Wessel, P., & Kroenke, L. W. (2008). Pacific absolute plate motion since 145 Ma: An assessment of the fixed hot spot hypothesis. *Journal of Geophysical Research*, *113*. https://doi.org/10.1029/2007JB005499

Wharton, M. R., Hathway, R., & Colley, H. (1995). Volcanism associated with extension in an Oligocene-Miocene arc, southwestern Viti Levu, Fiji. In J. L. Smellie (Ed.), *Volcanism associated with extension at consuming Plate Margins* (Vol. 81, pp. 95–114). Geologiical Society Special Publication.

Whelan, P. M., Gill, J. B., Kollman, E., Duncan, R. A., & Drake, R. E. (1985). Radiometric dating of magmatic stages in Fiji. In D. W. Scholl, & T. L. Vallier (Eds.), *Geology and offshore resources of Pacific Island Arcs; Tonga region* (Vol. 2, pp. 415–440). Circum-Pacific Council Energy and Minerals Resources.

Woodhall, D. (1985a). Geology of the Lau Ridge. In D. W. Scholl, & T. L. Vallier (Eds.), *Geology and offshore resources of Pacific Island Arcs-Tonga region*, *Circum-Pacific Council for Energy and Mineral Resources Earth Science Series* (Vol. 2, pp. 351–378). Circum-Pacific Council for Energy and Mineral Resources.

Woodhall, D. (1985b). *Geology of Taveuni, Qamea, Laucala, Cikobia, and adjacent islands (map)* (Vol. 802). MRD.

Woodhead, J. D., Hergt, J., Davidson, J. P., & Eggins, S. M. (2001). Hafnium isotope evidence for "conservative' element mobility during subduction zone processes. *Earth and Planetary Science Letters*, *192*, 331–346. https://doi.org/10.1016/s0012-821x(01)00453-8

Wysoczanski, R. J., Todd, E., Wright, I. C., Leybourne, M. I., Hergt, J. M., Adam, C., & Mackay, K. (2010). Backarc rifting, constructional volcanism, and nascent disorganized spreading in the southern Havre Trough backarc rifts (SW Pacific). *Journal of Volcanology and Geothermal Research*, *190*, 39–57. https://doi.org/10.1016/j.jvolgeores.2009.04.004

Yang, S., Humayun, M., & Salters, V. J. M. (2020). Elemental constraints on the amount of recycled crust in the generation of mid-ocean ridge basalts (MORBs). *Science Advances*, *6*, eaba2923. https://doi.org/10.1126/sciadv.aba2923

Zellmer, K. E., & Taylor, B. (2001). A three-plate kinematic model for Lau Basin opening. *Geochemistry, Geophysics, Geosystems*, *2*(4). https://doi.org/10.1029/2000GC000106

10.1029/2022GC010663

Erratum

The following errors were discovered after publication of this paper: Table 1 and Table 2 contained incomplete and incorrectly set information. These tables have now been replaced with complete, corrected Tables 1 and 2. This may be considered the authoritative version of record.